2

MOFs and Metal Oxides for Gas Adsorption and Environmental Applications

2.1 Introduction

Acid gases like carbon dioxide (CO_2) and hydrogen sulfide (H_2S) represent two most abundant harmful gases in the natural gas streams which need to be removed for achieving usefulness of natural gas. Similarly, environmental pollution due to the release of harmful gases from different industrial and household processes leads to severe degradation of the quality of air and significant efforts are required to minimize pollution level as well as to remove the pollutants from the environment. Some of the harmful materials that are present in our environment are H_2S, CO_x, SO_x, NO_x, nitrogen containing compounds (NCCs), sulfur containing compounds (SCCs), volatile organic compounds (VOCs), dyes, pharmaceuticals and personal care products (PPCPs).

2.1.1 Classification of Hazardous Materials

Depending on the sources, the most plentiful hazardous materials can be categorized into two classes, namely naturally originating hazardous materials and anthropogenic. A substantial quantity of naturally occurring materials are available underground as well as in water, soil, air and minerals. However, the anthropogenic materials generate from chemical reactions, combustion or from the effluent of toxic materials. The global energy need is satisfied by the naturally originating materials such as coal, crude oil and natural gas. As mentioned earlier, natural gas contains harmful gases like CO_2 and H_2S among others, which require removal. In addition, these energy sources when burnt generate high amounts of harmful gases to the atmosphere. The major toxic gases causing environmental air pollution are CO_2, H_2S, SO_x, NH_3, NO_x, VOCs and other hydrocarbons [1]. The gases like SO_2, CH_4, O_3 and N_2O are considered as greenhouse gases and the ejection of these gases enhances the ozone levels present in the troposphere. Vehicles related pollutants such as CH_4, CO, NO_2, SO_2 as well as carbon black also cause global warming. Currently, the carbon balance of the world is considered as one of the critical environmental

Haleema Saleem and Vikas Mittal, The Petroleum Institute (part of Khalifa University of Science and Technology), Abu Dhabi, UAE*
**Current address: Bletchington, Wellington County, Australia*

problem, and hence the reduction of anthropogenic CO_2 release has now become a very significant issue. VOCs are chemicals having high vapor pressure, and are usually discharged from adhesives, resins, paints, solvents, etc. [2]. Benzene, toluene, xylene and phenolics are some of the common hazardous VOCs. Nitrogen or sulfur containing organic compounds are naturally originating species, and are available in fossil fuels as well as oils like jet fuel, gasoline, crude oil, heating oil and diesel. The combustion of fossil fuels is a large source of toxic releases, which causes global warming, greenhouse effect, dangerous impact on living species and hazardous air pollution [3-5].

Further, due to the global industrial advancement, the severity of water pollution has become critical, thus, posing significant challenges to the health of living beings [6]. Dissolved heavy metal salts or organic pollutants are often present in the polluted water [7,8]. The organic pollutants existing in the natural water resources cause a great damage to the aquatic habitats and also to the human health. Some of the toxic pollutants existing in the waste water are benzene, phenols, nitro-benzenes, chlorinated benzenes, phthalates and chlorinated phenols. Dye materials are commonly used in plastics, textiles, paper and leather industries, and a large amount of these materials ends up in water as harmful pollutant [9,10]. Separation of these dyes from waste water is very crucial, but challenging. PPCPs are chemical contaminants that are present in water, and are also unsafe for living organisms and have to be removed [11]. The disposal of heavy metal ions like chromium (Cr), lead (Pb), copper (Cu), arsenic (As), mercury (Hg), antimony (Sb), cadmium (Cd) and manganese (Mn) in processed water is also highly toxic to human beings as well as ecological systems [12,13].

2.1.2 Adsorption of Hazardous Materials

In the last few decades, the porous materials have evolved as good adsorbents that exhibit significant potential for the purification of air, gas and water streams by adsorptive separation of the contaminants, and hence a great deal of research focus has been devoted for the examination and analysis of the advanced porous materials [14]. For the decontamination, adsorption has been regarded as the preferable technique due to its low cost, no or harmless secondary products, design simplicity, ease of operation and efficient adsorbent regeneration. This method is based on the porous adsorbent ability to selectively adsorb specific materials from either refinery streams or from the atmosphere. The adsorbent materials can be structurally tuned to generate suitable pore shape and size, thus, providing efficient contact with the adsorb-

ate materials, thus, leading to effective separation of pollutants during the adsorption process. Depending on the interaction between the porous sorbents and the adsorbates, the adsorbents can be classified as physical and chemical adsorbents [15]. With respect to physical adsorbents, the adsorbates are trapped inside the adsorbent pores through weak van der Waals forces. Hence, the adsorbent material can be easily regenerated by physical treatments or simple solvent exchange. However, in the chemical adsorbents, absorption takes place by the chemical bond formation between the adsorbent and the adsorbate. Therefore, chemical treatments are required for the regeneration of the spent adsorbents, which may also occasionally lead to permanent loss of adsorbent performance. The capability of the adsorption process depends on the selectivity for specific compounds, regenerability of adsorbents, durability and adsorption ability of the adsorbents. For the adsorptive removal of harmful compounds, different porous adsorbents like zeolites [16,17], activated carbons [18,19] , mesoporous materials [20,21] and metal organic frameworks (MOFs) [22,23] have been studied. For the effective adsorption, specific pore geometry, porosity and adsorption sites are needed [24]. In addition to this, certain active species such as different functional groups (basic or acidic), metal oxides, metal ions, polyoxometalates and metal salts are generally included into the adsorbents for the selective removal of harmful compounds by interactions such as hydrogen bonding, acid-base and π- π interactions.

In this chapter, the main focus is to elucidate the role of MOFs and metal oxides for the adsorptive removal of hazardous gases like H_2S, NH_3, CO_2, and other hydrocarbons present in the atmosphere as well as the dissolved heavy metal salts or the organic pollutants present in the polluted water. Beneficial characteristics of MOFs and metal oxides have been discussed that ensure their effective role in the adsorption of specific toxic compounds. The effect of linkers, open metal sites, MOF modification/functionalization, central metal ions and the adsorbent/adsorbate interactions are also explained. Further, the analysis of adsorption mechanisms such as electrostatic interactions, hydrogen bonding and acid-base interactions for the effective adsorption is also presented. Thus, this review presents an up-to-date study of theoretical predictions, experimental results as well as developing concepts on the adsorption ability of different MOFs and metal oxides, with specific emphasis on the removal of harmful gases like CO_2, H_2S, NH_3, and water contaminants like the heavy metals and organic contaminants, among other contaminants. In addition to this, observations in terms of benefits and disadvantages of employing different metal oxide frameworks as well as metal oxides have also been

pointed out, along with discussing in detail the thermodynamic and kinetic analysis.

2.2 Metal Organic Frameworks

MOFs consists of two major components, i.e., an organic molecule (linker) and a metal ion or a group of metal ions. The linkers are generally di-, tri- or tetradendate ligands [25]. Examples of some MOFs are Cu-BTC, MOF-5 and CPO-27. The porous MOFs are very attractive because of their versatile applications like CO_2 storage/adsorption [26], vapor adsorption [27], hydrogen storage[28], chemical separation [29], drug delivery [30] and so on. These materials are preferred than other porous materials due to their pore functionality, high and tunable porosity, pore compositions and open metal sites. For the adsorption related applications, MOFs are promising materials due to their controlled tuning of the pore surface, which causes the selective adsorption of certain guest molecules which have specific functional groups. The properties of the MOFs can be tuned for obtaining the desired performance, by orderly and intentionally tuning the functionalities and structures. Hence, many research studies have been carried out on the adsorption of different liquid and gaseous components using MOF, due to their beneficial features of pore geometry and porosity [31]. Depending on the adsorbates, both modified as well as virgin MOFs can be used for the adsorptive removal of different toxic gases and liquids.

2.2.1 Adsorptive Removal of Harmful Gases

Using different MOFs, adsorption of various harmful gases/vapors like H_2S [32,33], NH_3 [4], CO_2 [34,35], SO_2 [36], benzene [37], NO [38] have been studied. Most of the aforementioned gases/vapors are either required to be removed from products or are ejected from different industries as waste by-products. For a clean and safe environment, efficient removal of these harmful gases is very important. As mentioned earlier, MOFs have advantages like high porosity as well as easy tunability of pore shape and size, from mesoporous to microporous scale, by altering the nature of organic molecule and connectivity of inorganic component [39]. The characteristic examples include zirconium based MOFs namely UiO-68(Zr- terphenyldicarboxylate, Zr-TPDC), UiO-67 (Zr-BPDC, Zr- biphenyldicarboxylate) and UiO-66 (Zr- benzenedicarboxylate, Zr-BDC) having high surface areas 4170, 3000 and 1187 m^2/g respectively [40]. The large enhancement in the surface area is obtained by varying the or-

ganic linker. The following sections describe the specific use of MOFs for the removal of various harmful gases.

CO_2 Adsorption

The adsorption as well as desorption of CO_2 in MOFs are attributed to the variations happening in the framework structures, and have also been described using the "gate effect mechanism" or a "breathing type mechanism". In a further study, Walton *et al*. [41] added through the comparison of Monte Carlo simulation and experimental adsorption of CO_2 for MOF IRMOF-1 that attractive electrostatic interactions between the CO_2 molecules resulted in the unusual shape of the adsorption isotherms (Figure 2.1).

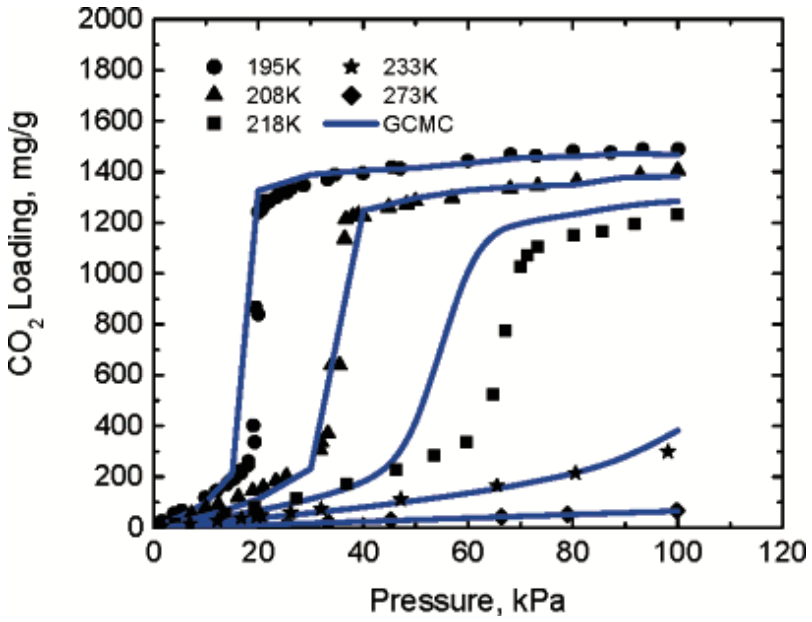

Figure 2.1 Comparison of Monte Carlo simulations (GCMC) and experimental adsorption isotherms for CO_2 in IRMOF-1. Reproduced from Reference 41 with permission from American Chemical Society.

For the application in flue streams, MOF adsorbents for the CO_2 capture should meet the requirements such as high CO_2 adsorption ability, corrosion resistance, high thermal stability and good selectivity for CO_2 over several other components present in flue gas. It should also be noted that most of these adsorbents exhibit little adsorption in the low-pressure conditions i.e. 0.1–0.2 bars, which is the realistic pressure range employed for the CO_2 adsorption from flue gas stream [42]. Further, a reduction in their adsorption capacity is seen when it exposed to gaseous mixtures under dynamic conditions.

Hence, significant efforts are required for the enhancement in the CO_2 adsorption capacity under equilibrium conditions. In this study, the modifications in MOFs was achieved in three aspects namely (1) metal ions, (2) organic linkers and (3) novel consolidation of both. As shown in Figure 2.2, the functionalized MOF was subjected to cyclic gas treatments. A small 0.75 wt% change in the weight of the sample was observed over repeated cycles, which confirmed that the material was able to withstand cyclic exposure to the mixed gas stream. The adsorption performance was maintained over the cycles and the material could be regenerated effectively.

For the metal ions, generating open metal sites is an effective method, as the vacant coordination sites at metal ions act as primary sites for the guest molecules [43]. Britt *et al*. [43] stated that MOF loaded with open Mg sites, Mg-MOF-74 (Mg2(2,5-dioxidoterephthalate)) had high selectivity, easy regeneration and excellent performance for the CO_2 removal. Mg-MOF-74 was exposed to a gas stream consisting of 20% CO_2 in CH_4, and the adsorbent was

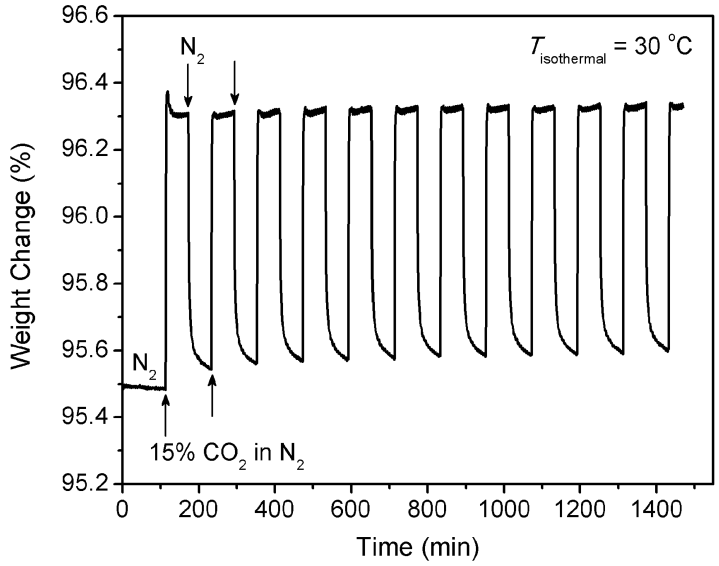

Figure 2.2 Gas cycling experiment for the functionalized MOF at 30°C, with 15% CO_2 in N_2 followed by a flow of pure N_2. Reproduced from Reference 42 with permission from American Chemical Society.

observed to capture CO_2 alone, without CH_4. The adsorbent retained 89 g of CO_2/kg of material prior to breakthrough (2.23 mmol.g^{-1}). Dietzel *et al*. [44] studied the outcome of the metal center on the CO_2 adsorption ability and selectivity using a series of iso-structural MOFs namely M-CPO-27s (M=Ni, Mn, Co, Mg, Zn). It was observed that at high pressure (50 bar) and 298 K, the CO_2 adsorption was 63 wt% for MOF CPO-27(Mg) and 51 wt% for the MOF CPO-

27(Ni). In another research by Caskey *et al*. [45], it was observed that at 1 atm, the CPO-27(Co) exhibited CO_2 adsorption of 30.6 wt%, whereas CPO-27(Mg) showed an adsorption of 35.2 wt%. The CO_2 adsorption ability of CPO-27(Mg) was found to be superior as compared to the other members of the series, thereby representing a major development in the CO_2 adsorption ability of the MOFs. In addition to this, for enhancing the performance, the unsaturated metal sites could be functionalized using groups like amine. Couck *et al*. [46] proved the efficient separation of CH_4 and CO_2 gases using amino functionalized MIL-53(Al). Due to the presence of quadrupole moment in CO_2, these CO_2 molecules have a greater affinity for the NH_2 groups. Breakthrough experiments confirmed that the CH_4, which was weakly adsorbed, was able to transmit through the MOF packed column during the adsorption of CO_2. Thus, at ambient conditions, effective separation of CO_2 and CH_4 could be achieved using the aforementioned MOF adsorbent.

For the organic linkers modification, Bae *et al*. [47] analyzed the feasibility of utilizing MOFs which are carborane based or coordinated with ligand mixture. A higher selectivity for CO_2 over CH_4 was noticed in these MOF materials. Carboranes have several beneficial material properties like thermal stability, rigidity and chemical stability. In the pursuit of preparing novel MOFs having high CO_2 adsorption capacity as well as stability, the capability to generate MOFs having different organic linkers as well as metal joints is considered to contribute significant flexibility, along with particular physical behavior and chemical functionalities. Recently, Yaghi *et al*. [48] prepared a new class of MOFs called zeolitic imidazole frameworks (ZIFs), where metal atoms like Zn were bonded with nitrogen atoms by ditopic imidazolate or functionalized Im links to generate the neutral frameworks. The materials had good chemical as well as thermal stabilities (until 500 °C). In another study by Phan *et al*. [49], it was stated that at 0 °C, 1 L of ZIF-69 had the ability to store 82.6 L of CO_2. Further, ZIFs also exhibited higher selectivity than other MOF types for the adsorption of CO_2 from flue gases. It was found that only CO_2 could slip into the ZIF cages, whereas other gas molecules could just pass through them without any obstruction.

Hu *et al*. [50,51] studied the effect of addition of alkaline metal cations like Na^+, Li^+ and K^+ into a previously studied Zr-MOF having excellent CO_2 adsorption properties, by facile neutralization reactions. The CO_2 adsorption capacity of the MOFs was analyzed employing breakthrough experiments and sorption isotherms. From the binary mixed gas breakthrough experiment, it was seen that out of the different Zr-MOFs, the MOF UiO-66 (Zr)-$(COONa)_2$ exhibited high CO_2/N_2 selectivity value of 99.6. This was considered to be highest among

all the previously obtained values under analogous testing conditions. The MOFs were reported to have good CO_2 adsorption capacity, high water stability and excellent CO_2/N_2 selectivity. Further, their preparation could be scaled up very efficiently by utilizing commercially accessible reagents with batch reactors as well as environmental friendly solvent like water. The results obtained in the study confirmed that the synthesized MOFs are very efficient adsorbents for the removal of CO_2 from flue gas. Yang *et al*. [52] observed enhanced CO_2 adsorption with adsorbents attained by sonication or microwave heating. At 298 K, the small sized and homogenous particles of CPO-27(Mg), generated by sonication method, adsorbed almost 350 $mg.g^{-1}$ of CO_2. In addition to this, the materials also exhibited large isosteric heat of adsorption. Table 2.1 also demonstrates the CO_2 adsorption capacities of some of the MOFs.

Table 2.1 Comparison of CO_2 adsorption capacities of some of the MOF adsorbents

Sl. No.	Adsorbent	Temperature	Pressure	CO_2 adsorption capacity (wt%)	Reference
1	CPO-27(Mg)	298 K	50 bar	63 wt%	131
2	CPO-27(Ni)	298 K	50 bar	51 wt%	131
3	CPO-27(Co)	Ambient temperature	1 atm	30.6 wt%	132
4	CPO-27(Mg)	Ambient temperature	1 atm	35.2 wt%	132

Adsorption of Sulfur Containing Compounds

The use of fossil resources, like petroleum, natural gas and coal, generates sulfur containing species like SO_2, H_2S, mercaptan, thiophene and thioether. These sulfur containing compounds are harmful to human health and the environment and hence the desulphurization processes are needed. As mentioned earlier, MOFs are also promising absorbents for the removal of sulfur containing comounds. In a study by Achmann *et al*. [53], it was noted that the adsorbent MOF-199 possessed high efficiency for the removal of sulfur from low sulfur model fuels and oil. The MOF also exhibited the maximal sorption rates as well as rapid sorption characteristics. The minor pores in the MOF-199 provided better stabilization for Cu- adsorbed sulfur species by the van der Waals force, and thereby caused an excellent sulfur adsorption performance. In another study, Chavan *et al*. [54] analyzed the H_2S adsorption performance on the adsorbent Ni-MOF-74. The adsorbent exhibited maximal uptake and

higher H_2S adsorption enthalpy, when compared to other adsorbents, while preserving its original porosity and structure (Figure 2.3).

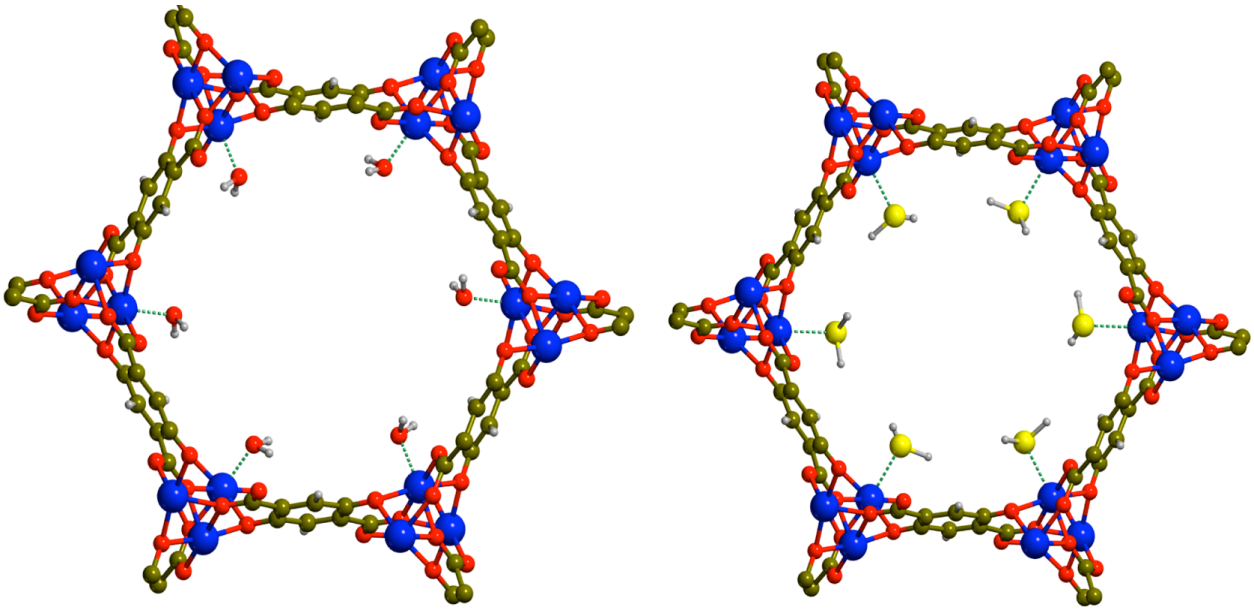

Figure 2.3 H_2O (left) and H_2S (right) molecules as arranged in the CPO-27-Ni channels. Reproduced from Reference 54 with permission from American Chemical Society.

In a study reported by de Voorde *et al*. [55], DFT analysis on the adsorption behavior of S-heterocyclic compounds on MOF-74 series (Mg, Cu, Ni, Zn and Co) was carried out. It was confirmed that the metal ion had a remarkable effect on the MOFs adsorption ability and S-heterocyclic species affinity. It was suggested that the adsorbent Ni-MOF-74 offered the best desulfurization behavior. Hamon *et al*. [56] examined the efficiency of MIL-series e. g. MIL-100(Cr), MIL-53(Cr, Fe and Al), MIL-101(Cr) and MIL-47 for the adsorption of H_2S at 303 K. The study suggested that the –OH groups present in the MIL-53 adsorbent promoted the H_2S adsorption. In a different study by Hamon *et al*., [57] it was reported that the –OH groups existing in the MOFs performed as proton donor, thereby increasing the H_2S adsorption. The authors observed that on H_2S adsorption, the MIL-47(V) structure remained rigid up to a pressure of 1.8 MPa. On the other hand, the MIL-53(Cr) initially present in the large pore form (LP) switched to its narrow pore version (NP) at very low pressure, and exhibited a second structural transition from the NP to the LP at higher pressure. The authors observed that experimental and simulated adsorption enthalpies for H_2S decreased in the sequence: MIL-53(Cr) NP > MIL-47(V) > MIL- 53(Cr) LP, also depicted in Figure 2.4.

Several previous studies have showed that the efficiency of MOFs can be influenced by the factors such as metals ions, substituent groups and coordinatively unsaturated sites (CUS). Further, most of the studies were based on the adsorption of thiophene species from liquid fuel. Chen *et al*. [58] performed research on the desulfurization ability of MOFs for the H_2S, mercaptan and thioether species. A systematic DFT analysis on the influence of MOFs metal centre (structures as well as metal ions) and organic ligands on the adsorption of H_2S, CH_3SCH_3 and CH_3CH_2SH was carried out. It was noted that the desulfurization ability of MOF-74 and MOF-199 with open metal site, was superior to the other MOFs without coordinatively unsaturated sites. The observation confirmed the remarkable influence of CUS on the sulfur compounds adsorption. Here, IRMOF-3 containing amino groups exhibited the maximal sulfur

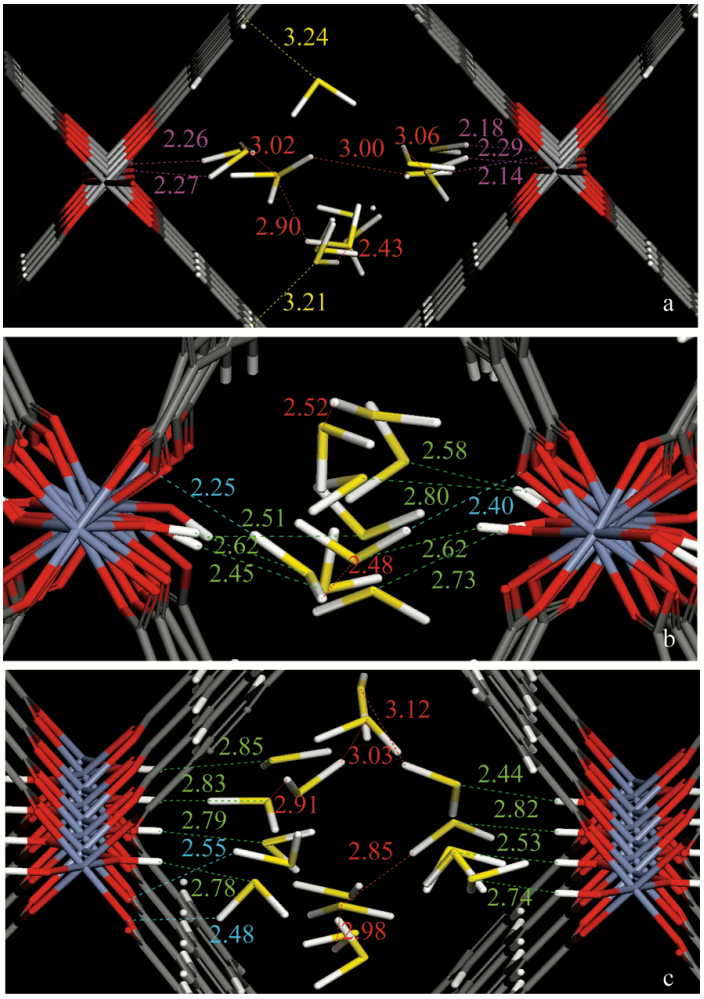

Figure 2.4 Illustrations of the preferential arrangements for H_2S simulated at 303 K in MIL-47(V) (a), MIL-53(Cr) NP (b) and MIL-53(Cr) LP (c) solids. Reproduced from Reference 57 with permission from American Chemical Society.

capacity, succeeded by IRMOF-8. However, it was noted that the density of CUS sites present in the Zn-MOF-74 (6.16×10^{-3} mol/g) was greater than Cu-MOF-199 (4.96×10^{-3} mol/g), and hence the sulfur removal ability of Zn-MOF-74 was confirmed to be lesser than that of Cu-MOF-199. Fernandez *et al*. [59] studied the adsorptive removal of toxic acid gases by using fluorinated MOF (FMOF-2), which was prepared using zinc nitrate hexahydrate and 2,2'-bis(4-carboxyphenyl) hexafluoropropane. The MOF was observed to be stable for the H_2S and SO_2 adsorption. With FMOF-2, the estimated weight capacities for H_2S and SO_2 were 8.3% and 14% respectively, at 1 bar and room temperature. Dathe *et al*. [36] studied the SO_2 adsorption using $Ba(CH3COO)_2$ (or $Ba(NO_3)_2$ and $BaCl_2$)-impregnated Cu-BTC. The impregnation accelerated the formation of small micro-crystals of barium salts in Cu-BTC pores. Also, the sectional destruction of the host structure took place in $BaCl_2$. It was also noticed that at greater temperature, the SO_2 adsorption surpassed the stoichiometric ability based on Ba^{2+} concentration. Accordingly, the excess SO_2 adsorption was because of the chemical bonding between the SO_2 and metal cations, thereby resulting in the generation of Cu-sulfates. Hence, at lower temperature, Cu-BTC performed as an excellent host material for obtaining very well dispersed barium salts. However, at higher temperature, the adsorbent Cu-BTC decomposed and generated unique Cu species that performed as SO_x storage sites, thus producing Cu-sulfates finally. Thus, the main limitation of these bariums salts impregnated Cu-BTC adsorbent is the irreversible SO_x storage in their structure.

Adsorption of Other Harmful Gases

For the adsorption of various toxic gases, the open metal sites of MOFs have been stated repeatedly as the active sites. Further, a large number of studies stated that the properties of MOFs could be controlled by the loading of active metals (Pd, Cu or Ag) or active species (sulfated zirconia or polyoxymetalates) or by generating composites [60]. Glover *et al*. [61] demonstrated the adsorption of various toxic gases like SO_2, NH_3, octane vapor and CNCl using M-CPO-27 (M=Zn, Ni, Mg or Co) under humid and dry conditions. The breakthrough results confirmed that only under the dry conditions, the adsorbents with open metal sites were able to adsorb the aforementioned toxic gases. In humid conditions, the adsorptive ability decreased significantly as the aggressive adsorption of water started dominating. In the case of NH_3, the reduction in the adsorption capacity was not identified, as it was adsorbed similarly under both humid and dry conditions. Hence, it could be confirmed that the presence

of water vapour had a negative influence on the adsorption of different toxic gases using the CPO-27 type adsorbents.

Petit and Bandosz [62] studied different composites of MOFs (MIL-100(Fe), MOF-5 or Cu-BTC) and graphitic compound (GO, graphite or graphite oxide), under ambient conditions, for the adsorption of NO_2, H_2S and NH_3. It was observed that the open metal sites of MOFs coordinated with oxide groups of GO, which caused the generation of a new pore space in the interface between the MOF units and carbon layers, to form composites having definite properties. With the GO/Cu-BTC composites, more than 50% (for H_2S), 12% (for NH_3) and 4% (for NO_2) enhancement in the adsorption ability was observed. The increase in the adsorption ability for the toxic gases seen in the composites was attributed to the porosity generated in the interface where the dispersive forces were substantial. Britt *et al*. [63] studied the possible suitableness of six MOFs, consisting of 2-amino terephthalate (IRMOF-3), diacetylene-1,4-bis(4-benzoic acid) (IRMOF-62), $Zn_4O(CO_2)_6$ group linked by terephthalate (MOF-5), benzene-1,3,5-tris(4- benzoate) (MOF-177), Cu-BTC and $Zn_2O_2(CO_2)_2$ chains linked by 2,5-dihydroxyterephthalate (CPO-27), for the adsorption of different hazardous gases/vapors including NH_3, chlorine, SO_2, benzene, tetrahydrothiophene and ethylene oxide. The obtained results were correlated with BPL carbon. It was seen that different factors like the active adsorption site having specific functional group and open metal sites of Cu-BTC or CPO-27 played a critical role in deciding the dynamic adsorption ability of these MOFs. Compared to the other MOFs, CPO-27 exhibited excellent performance, and the adsorption ability was almost 6 times higher than the BPL carbon. The improved adsorption was because of the existence of an immensely reactive 5 coordinate Zn species, together with the reactive oxo-group present in CPO-27. However, in the case of all other gases except Cl_2, the MOF Cu-BTC exhibited higher efficiency than BPL carbon. For NH_3 adsorption in IRMOF-3, the existence of NH_2 in the MOF greatly increased the adsorption ability, when compared to MOF-5 or IRMOF-1. Prior to the breakthrough, the IRMOF-3 adsorbed NH_3 approximately 71 times, when compared to the BPL carbon, due to the ability of NH_3 to easily form the hydrogen bonds.

CO, another toxic gas in the environment, has good binding capacity with the metal sites and MOFs with CUS can easily adsorb CO from gaseous mixture. Karra and Walton [64] conducted molecular simulation analysis and observed that at 298 K, Cu-BTC was a good adsorbent for CO over N_2 and H_2. It was proposed that the electrostatic interaction between the CO dipole and partial charge of CUS of Cu-BTC controlled the adsorptive behavior. Different MOF materials can also be used successfully to adsorb NO by adsorption pro-

cesses [65]. The gravimetric NO adsorption on the open metal sites of Cu-BTC at 196 K and 1 bar was examined by Xiao *et al*. [65]. It was observed that by using 1 g of Cu-BTC almost 9 mmol of NO was adsorbed, which was remarkably greater than any other porous solids for the NO adsorption (Figure 2.5). The adsorption of benzene (both liquid and vapor phase) was also analyzed by Jhung *et al*. [66] using MIL-101(Cr), chromium terephthalate adsorbent. 16.7 mmol.g^{-1} of benzene (vapor phase) was adsorbed by the adsorbent MIL-101(Cr). The obtained value was approximately 8.7, 5.5 and two times higher than the H-ZSM-5, SBA-15 and a commercial activated carbon, respectively. Due to the high porosity of MIL-101(Cr), it displayed higher benzene adsorption capacity than the pitch based activated carbon (12.4 mmol.g^{-1}) with a higher surface area of 2600–3600 m^2 g^{-1}. The potential utilization of MIL-101(Cr) in the vapor phase adsorption of VOCs like p-xylene and ethyl acetate was also studied by Shi *et al*. [67].

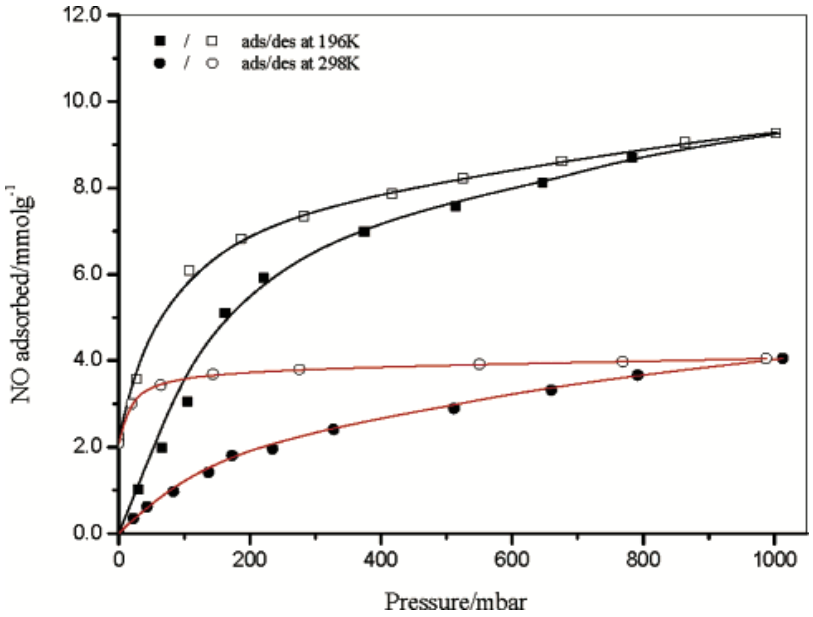

Figure 2.5 Adsorption (filled symbols) and desorption (open symbols) isotherms at 196 K (squares) and 298 K (circles) for nitric oxide on HKUST-1. Reproduced from Reference 65 with permission from American Chemical Society.

2.2.2 Adsorptive Elimination of Contaminants from Wastewater

Various MOFs have been employed for the adsorption of different hazardous contaminants from water. The adsorption occurs through different mechanisms like the electrostatic interactions, hydrogen bonding, acid-base interac-

tions, hydrophobic interactions and π-π interactions. One of the substantial barrier for the application of several types of MOFs is the water instability (both in vapour and liquid phase). This instability of MOFs in water is a critical problem and many research studies have been carried out to increase their water stability [68]. Computational as well as experimental studies showed that several MOFs like MIL-101-V, MOF-5 experienced degradation by ligand displacement, when these materials were exposed to water [69,70]. On the other hand, MOFs like UiO-66 [71], ZIF-8 [72] MIL-101-Cr [73], MIL-100 (Fe, Al, Cr) [74,75] had good water stability and were suitable for the adsorption application in water or water purification. Several methods like incorporation of water repellent functional groups [76], composite formation [77] and fluorination [78] have been achieved to improve the water stability [79].

Haque *et al*. [80] reported the adsorptive separation of dye using MOFs. The authors utilized two types of porous Cr based MOFs, namely MIL-53-Cr and MIL-101-Cr, for the adsorption of methyl orange (MO), an anionic hazardous dye, from the aqueous solution. It was noticed that the performance of the MOFs was superior to the activated carbon. The adsorption kinetic constant and the adsorption capacity of MIL-101-Cr were higher than that of MIL-53-Cr, thereby portraying the significance of pore size as well as porosity for the adsorption. On the other hand, a better adsorption was seen after the functionalization of MIL-101-Cr with ethylenediamine (ED) and protonated ED (PED). Generally, MO exists in the sulfate form, and hence it exhibits greater electrostatic interaction with an adsorbent having positive charge. It was observed that the positive charge dispersion enhanced in the order MIL-101-Cr < ED-MIL-101-Cr < PED-MIL-101-Cr. On the other hand, the positive charge on PED-MIL-101-Cr reduced with enhancing the solution pH, due to the deprotonation of the protonated adsorbent. In another study, Haque *et al*. [81] analyzed the adsorption of methylene blue (MB-cationic) and MO from aqueous solution, using NH_2-MIL-101-Al, an NH_2-functionalised MOF. The ultimate adsorption ability of NH_2 -MIL-101-Al, for the removal of MB was observed to be 762±12 mg/g at 30 °C, which was higher than most other porous materials and MOFs. However, by using non-amine functionalized framework (MIL-101-Al), lower adsorption capacity was noticed (195 mg/g). Thus, it suggested that the electrostatic interactions between the cationic MB and the amino groups of the MOF favored the adsorption. Haque *et al*. [82] also reported that the iron terephtahalate MOF (MOF-235) could adsorb both the cationic (MB) as well as anionic (MO) dyes from the waste water. Here, the adsorption kinetic constant and adsorption capacity of MOF-235 were higher as compared to that of the activated carbon. The higher adsorption of MB or MO was ex-

plained on the basis of the electrostatic interactions between the adsorbents and dyes. MB existed in positive form and MO existed in negative form, and hence electrostatic interactions were observed with the adsorbents having negative (charge balancing anion) charges as well as positive framework respectively. After the equilibration with MOF-235, MB and MO adsorptions at varying pH values were determined. By increasing the pH of the MO solution, it was observed that the quantity of adsorbed MO reduced, as the positive charge density reduced with increasing pH. However, the quantity of adsorbed MB increased with pH increase, as the negative charge concentration increased with pH increase. In another study, Leng *et al*. [83] analyzed the adsorption behavior of uranine using MIL-101-Cr and observed the aforementioned type of interactions. The adsorptive removal ability of uranine using MIL-101-Cr was found to be 126.9 mg/g, which was much higher than the activated carbon (17.5 mg/g). This was due to the electrostatic interactions, which were explained by the zeta potential analysis. The zeta potential of MIL-101-Cr was observed to be around 21.1 mV, and zeta potential reduced to 12.0 mV after the uranine interaction. Chen *et al*. [84] studied the xylenol orange (XO) adsorption on MIL-101-Cr and observed significant adsorption ability of the material. It was observed that the enhancement in the pH of the solution decreased the amount of adsorbed XO. No adsorption was observed, when the pH of the solution attained 12. Thus, after the analysis of zeta potential, the authors concluded that the interactions between the adsorbent and dye played a key role in the adsorption process.

Hydrogen bonding also has a major role in adsorption of harmful materials using MOFs. Liu *et al*. [85] examined the adsorption of phenol and para-nitrophenol (PNP) from aqueous solution, using different MOFs (NH_2-MIL-101-Al and MIL-100-Fe, Cr). During the phenol adsorption, limited as well as similar adsorption ability was exhibited by all the three MOFs. On the other hand, NH_2-MIL-101-Al exhibited very high adsorption of PNP, which was about 1.9 times and 4.3 times greater than the MIL-100-Cr and MIL-100-Fe, respectively. The significant adsorption ability of NH_2-MIL-101-Al was because of the hydrogen bonding between the PNP and NH_2 groups in NH_2-MIL-101-Al, as illustrated in Figure 2.6. Xie *et al*. [86] examined nitrobenzene adsorption from waste water using two types of aluminum based MOFs, namely MIL-68-Al (1130 ± 10 mg/g) and CAU-1 (970 ± 10 mg/g). The adsorption values were greater than the experimental values reported for other porous materials. The two MOFs had μ-OH groups in Al-O-Al units, which played a crucial role in attaining higher adsorption by the generation of hydrogen bonding between the nitrogen atom in nitrobenzene and μ-OH groups of MOFs.

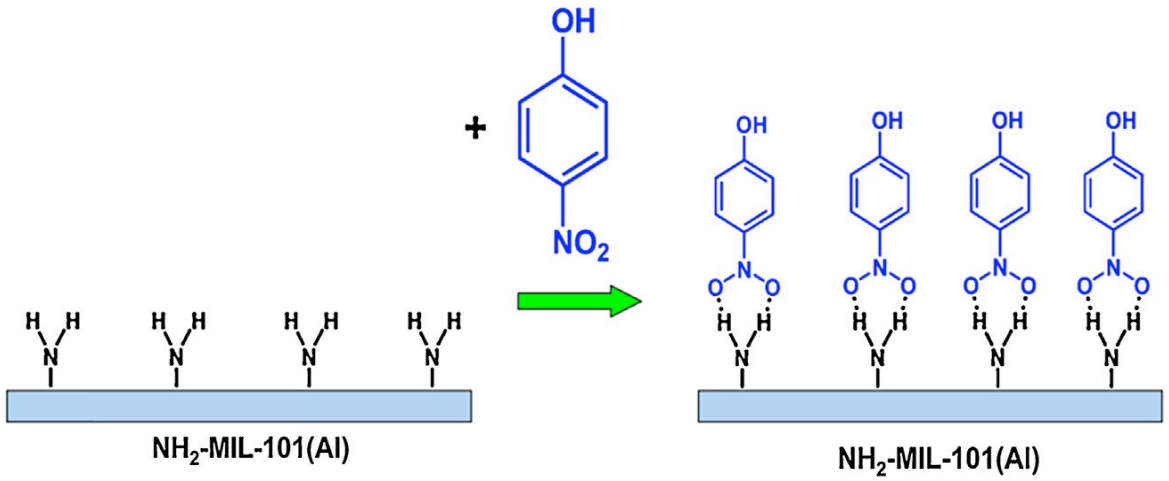

Figure 2.6 Mechanism of PNP adsorption on NH2-MIL-101-Al by hydrogen bonding. Reproduced from Reference 85 with permission from American Chemical Society.

Khan *et al*. [87] studied the adsorption of phthalic acid from water using ZIF-8 and other MOFs like NH_2-UiO-66, MIL-53-Cr, UiO-66, NH_2-MIL-100-Cr, MIL-100-Cr and MIL-100-Fe. When compared to other MOFs, the ZIF-8 exhibited higher adsorption at high pH. This might be due to the electrostatic interactions between the ZIF-8 (positive charged surface) and PA^{2-} as well as H-PA^{-} ions. Further, it was also obserevd that the amine functionalized MOFs exhibited higher adsorption of phthalic acid at lower pH, than the MOFs without NH_2 group. At low pH, the phthalic acid did not deprotonate, and the acid-base interaction between the basic sites and phthalic acid exhibited dominancy. Tong *et al*. [88] studied the effect of framework metal ions in the adsorption of dyes using MIL-100-Fe/Cr. The adsorbents MIL-100-Cr and MIL-100-Fe had identical pore volumes (0.75 cm^3/g and 0.76 cm^3/g) as well as surface areas (1760 m^2/g and 1770 m^2/g). On the other hand, it was noticed that both the MOFs exhibited different behavior for the adsorption of MB and MO from wastewater. For the adsorption of MO, the absorbent MIL-100-Fe displayed excellent adsorption (1045.2 mg/g), when compared to the adsorbent MIL-100-Cr (211.8 mg/g). Due to the greater binding energy of water molecules with the metal sites of MIL-100-Cr, the aggressive adsorption of water and MO was more outstanding at the MIL-100-Cr surface. The adsorption of water molecules occurred at the apertures of hexagonal and pentagonal windows, which limited the accessibility of MIL-100-Cr cages for MO to a higher degree. Size selective adsorption is also noticed during adsorption using MOFs. Wang *et al*. [89] analyzed the size selective adsorption of dyes having different sizes, where neutral MOFs were used for the adsorption. The MOFs had face centered cubic topologies with 3-dimensional frameworks, and were used for the

adsorption of three different dyes, i.e, MB, MO and rhodamine (RB). It was noticed that MB and MO were adsorbed, however, RB was not adsorbed due to its larger size that blocked the transmission through the smaller windows of the MOFs.

Presence of uranium in water is one of the most serious means of hazard to human health [90]. Adsorption is considered as the best method for the uranium removal from water due to its design flexibility, low cost and toxic pollutant insensitivity. Feng *et al*. [91] examined uranium adsorption capacity of the MOF HKUST-1 from aqueous solution. The most advantageous adsorption conditions were fixed along with the adsorbent dosage (0.03g), solution pH (at 6) as well as the agitation time (2 h). It was noticed that when the initial concentration of uranium was less than 200 mg/g, the temperature had no visible effect on the adsorption. However, when the initial concentration of uranium exceeded 200 mg/g, a greater temperature favored the adsorption process. At 318 K, the adsorbent HKUST-1 displayed an excellent adsorption capacity, at initial uranium concentration of 800 mg/L and solution pH value of 6. Further, the endothermic and impulsive nature of the adsorption process were indicated by the thermodynamics of HKUST-1/uranium system.

2.3 Metal Oxides

Transitional metal oxide nanoparticles have been adequately researched because of the attractive behavior as advanced nanomaterials in environmental as well as energy areas due to their excellent adsorption performance [92,93]. As mentioned earlier, harmful gases pose serious challenges to the process industries as well as environment. Wastewater from food processing, pharmaceutical and textile industries has constantly been a crucial environmental issue, as the contaminants have adverse effects on aquatic life as well as human health. Several dyes as organic contaminants are stable and difficult to degrade in conventional wastewater treatment methods. Thus, establishing effective and beneficial adsorption methods are needed for removing the organic contaminants present in the wastewater [94]. Metal oxide based adsorbents confirmed to be an efficient solution for the removal of a wide variety of contaminants. These oxides are available in various shapes and sizes, in the form of micro-particles, nanoparticles, nanocomposites and granules, thereby demonstrating distinct characteristics which are critical to their sorption properties. Several research studies have been carried out during the last two decades for developing various optimum methods of preparation of metal oxide adsorbents. Out of the different methods, thermal decomposition and re-

duction, sol–gel processes and hydrothermal preparation [95] are the most promising ones.

2.3.1 Adsorption of CO_2

In addition to the removal of CO_2 from natural gas, the removal of CO_2 from the large CO_2 emission sources like thermal power plants has also a significant role for preventing the global warming [96]. For the efficient removal of CO_2 using solid adsorbents, higher selectivity of CO_2 against other gases like nitrogen is very important. Chemical adsorption of CO_2 is considered as one of the methods to enhance the selectivity of the adsorbents. The metal oxides display improved selectivity due to the chemical adsorption between the CO_2 molecules and their surfaces. Chemical adsorption also allows the metal oxides for CO_2 adsorption in the existence of water vapor. H_2O undergoes physical adsorption and hence it has limited effect on the CO_2, which is adsorbed chemically. This behavior is different from zeolites, which are noted to have higher loss of CO_2 in the presence of water vapor. Together with the high selectivity for CO_2, the high surface area of the adsorbent is also very important for the efficient adsorption. The advancements in nanostructure control have facilitated the preparation of oxides with higher surface area by generating nanoparticles and porous structures. The utilization of these methods allows added enhancement in the CO_2 adsorption ability of the metal oxides.

Cai *et al*. [97] explored the synthesis of mesoporous alumina (MA) and MA-supported metal oxides. Aluminum isopropoxide, aluminum chloride, and aluminum nitrate nonahydrate were used as aluminum precursors, whereas nickel, magnesium, iron, chromium, copper, cerium, lanthanum, yttrium, calcium, tin chlorides, or nitrates were metal precursors. The authors observed that the use of aluminum nitrate nonahydrate for the synthesis led to large mesopores with size ranging from ~7 nm to 16 nm, improved ordering of the oxides as well as improved adsorption affinity toward CO_2. Figure 2.7 shows the temperature-programmed desorption (TPD) profiles of the <A and MA supported metal oxide materials for CO_2. The profiles exhibited a broad peak, which indicated the presence of a wide range of basic sites on the surface of these materials.

In another study, Leon *et al*. [98] studied magnesium-aluminum double oxides derived from the thermal treatment of layered hydroxides for CO_2 adsorption. The authors analyzed the effects of various factors, such as the incorporated cation (K or Na), mode of addition of precursors, sonication, and calcination temperature, and related these with the adsorption capacity by the

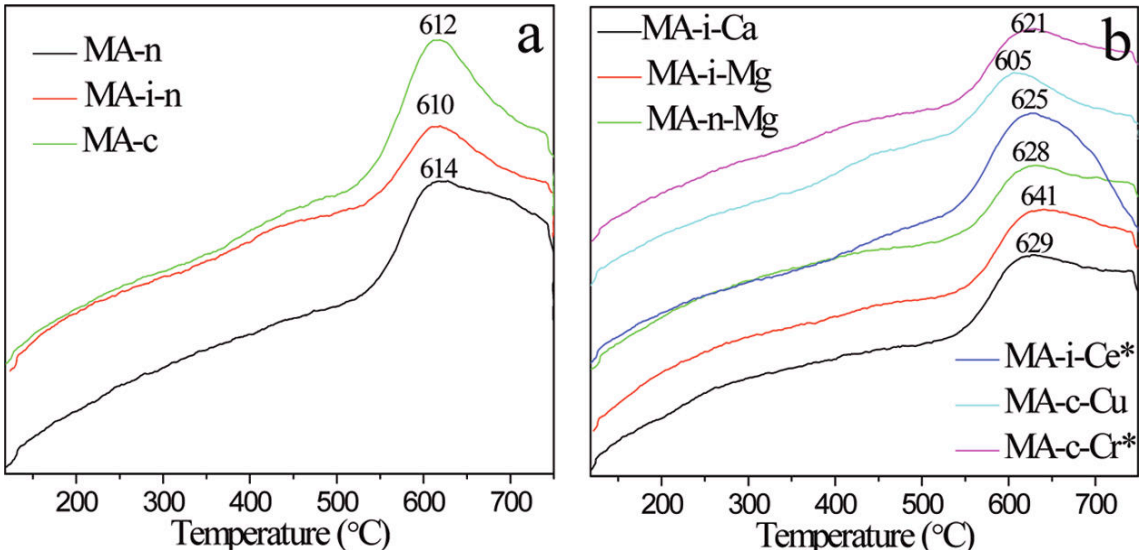

Figure 2.7 CO_2-TPD profiles for (a) MAs and (b) MA supported-metal oxides. Reproduced from Reference 97 with permission from American Chemical Society.

use of thermogravimetry and calorimetry. As observed in Figure 2.8, the equilibrium adsorption isotherms at 6.7 kPa and 323 K of the mixed oxides, recorded using microcalorimetry, exhibited the presence of combined chemisorption and physisorption behavior. It was observed that Langmuir transformation fit of the curves was achieved at low coverages, however, did not fit the data at higher extent of coverage, thus, indicating multilayer adsorption.

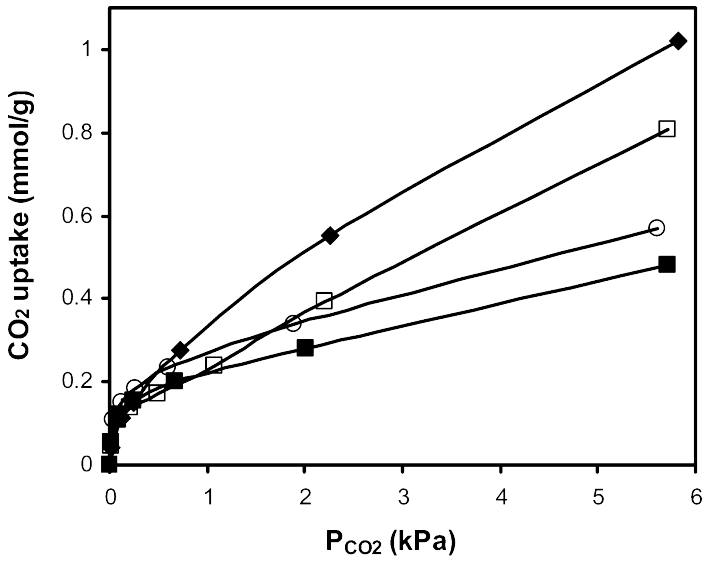

Figure 2.8 CO_2 adsorption isotherms at 323 K and 6.7 kPa, measured by microcalorimetry for (⧫) 1K723F, (□) 2K723F, (■) 1KUS723F, and (○) 2KUS723F. Reproduced from Reference 98 with permission from American Chemical Society.

Yoshikawa *et al*. [99] also studied the CO_2 adsorption behavior of single metal oxides. CeO_2, Al_2O_3, SiO_2 and ZrO_2 were generated, and the chemically adsorbed CO_2 amount was measured using CO_2 pulse injection. From the adsorption analysis, it was observed that the CeO_2 based adsorbents exhibited the highest CO_2 adsorption capacity. The temperature programmed desorption investigation of CO_2 confirmed that the CO_2, adsorbed on the CeO_2, got desorbed mostly at temperatures from 323K to 473 K, with the peak at 393 K. Further, a very small amount of desorption remained till the temperature reached 723 K. For analyzing the CO_2 adsorption as well as desorption mechanisms, the amount of CO_2 adsorbed on CeO_2 and the temperature dependence were examined with the help of FTIR spectroscopy. The FTIR analysis results confirmed that the hydrogen carbonate and bidentate carbonate species were essentially formed on the CeO_2 adsorbent surface. The lowest decomposition temperature was exhibited by the hydrogen carbonate species, which revealed that this species could be utilized to reduce the energy consumption for the capture of CO_2. It was also noted that for increasing the hydrogen carbonate, treatment with water vapor proved to be efficient. As the exhaust gases from the thermal power plants consist of CO_2 and water vapor, it has the ability to help the generation of hydrogen carbonate species. Hence, CeO_2 can be considered as an efficient adsorbent for the CO_2 adsorption in thermal power plants. Wang *et al*. [100] also studied high-temperature adsorption of CO_2 on mixed oxides, which were derived from hydrotalcite-like compounds. The oxides were characterized with various physicochemical techniques such as x-ray diffraction analysis, Fourier transform infrared spectroscopy, thermogravimetric analysis and BET. It was observed that the generated oxides were of either periclase or spinel phase, with an interparticle pore diameter of 9.6-15.4 nm. The oxides were observed to exhibit high CO_2 adsorption capability at 350 °C. For instance, mixed oxide CaCoAlO was observed to adsorb 1.39 mmol/g of CO_2 (6.12 wt%) from a gas mixture (8% CO_2 in N2) at 350 °C and 1 atm. The range of adsorption for other mixed oxides was 0.87–1.28 mmol/g (3.83–5.63 wt%) of CO_2. Figure 2.9 also demonstrates the CO2 adsorption data in the fixed bed reaction, in comparison with the simulated breakthrough curves.

In other studies for CO_2 adsorption, Zhao *et al*. [101] synthesized MgO nano/micro-particles with various morphologies as well as porous structures and studied the CO_2 adsorption ability of these porous materials. Song *et al*. [102] analyzed the CO_2 adsorption kinetics of MgO adsorbent under various CO_2 partial pressures and adsorption temperatures. The adsorption behaviors of MgO were successfully predicted by the pseudo-second order models. The

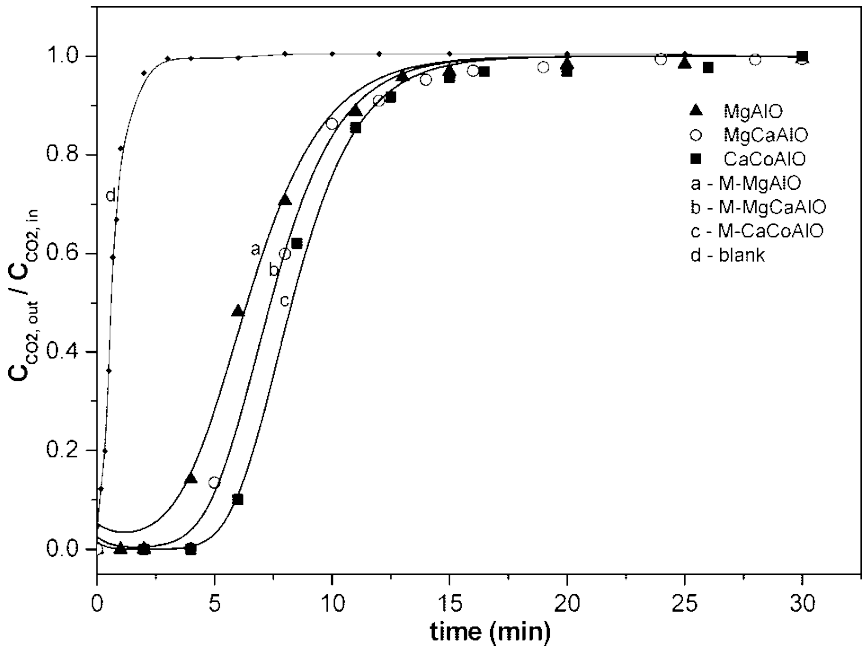

Figure 2.9 CO_2 sorption data in the fixed-bed reactor and simulated breakthrough curves. "M-" represents predicated curves. Reproduced from Reference 100 with permission from American Chemical Society.

material exhibited two stage process of adsorption, having a fast initial step succeeded by a sluggish second step. The first step was due to the diffusion of film from the bulk gas phase to the MgO exterior, whereas the second slow step was attributed to the strong inter-particle diffusion resistance due to the large number of narrow pores, thus, reducing the diffusion rate of CO_2. From the pore size and the pore area distribution, it was noted that the surface area of the generated MgO primarily located in small pores under 3 nm, where the CO_2 molecules underwent strong diffusion resistance. The study confirmed that the slow diffusion of CO_2 in the narrow pores reduced the MgO adsorption kinetics in spite of the fact that numerous pores contributed to larger surface area. Thus, it was revealed that an outstanding chemical adsorbent should have greater surface area for chemisorption as well as suitable pore size distribution for promoting the diffusion of CO_2 in the adsorbent porous structure. Kumar *et al*. [103] analyzed the CO_2 adsorption ability of mesoporous MgO, which acted as a promising pre-combustion CO_2 adsorbent. It was observed that at 350 °C temperature and CO_2 pressure of 10 bar, almost 96.96% of MgO changed to $MgCO_3$. In another study by Vu *et al*. [104], mesoporous MgO adsorbent was synthesized using aerogel technique and analysis of the CO_2 adsorption behavior at intermediate temperature range of 250–400 °C was carried out. At 325 °C and 120 min, the MgO sample exhibited higher

adsorption capacity of 13.9 wt%. Thus, it was confirmed that MgO exhibited higher CO_2 adsorption ability after modification and had the potential of being an excellent adsorbent for CO_2 removal.

Yu-Dong *et al*. [105] examined the CO_2 adsorption efficiency of MgO adsorbent in the presence of water vapor in a fixed bed. Initially, the analysis of CO_2 adsorption capacity of MgO adsorbent under dry condition was carried out. At 100 mL/min flow rate, it took almost 14 min for the CO_2 concentration of the outlet to reach 14.5%. A decrease in the time to reach the equilibrium was seen with the increased flow rate and it took just 4 min for that of 300 mL/min to obtain equilibrium. It was found that at 50 °C, with the increase in relative humidity from 30% to 70%, the CO_2 adsorption ability of MgO adsorbent enhanced from 0.82 mol/kg to 3.42 mol/kg. At a concentration of water vapor of 8.547% v/v and at an adsorption temperature of 75 °C, the CO_2 adsorption capacity reached a maximum value of 3.54 mol/kg. It was reported that the CO_2 adsorption efficiency of MgO was greatly dependent on the presence of water vapor. However, the time to obtain equilibrium increased because of the controlled diffusion of CO_2 arising due to the condensation of water vapor. The results obtained from the cycle experiments confirmed that the condensed water increased the aggregation of MgO particles. Further, it was also noted that at higher temperature, i.e., 100 °C, no water vapor condensation took place and the porous structure remained stable during the cycling adsorption. Elimination of the porous structure degradation and enhancement in the CO_2 adsorption capacity was observed at adsorption temperature between 100 °C and 110 °C. The study confirmed that MgO adsorbent could be developed as a promising material for CO_2 adsorption from wet flue gas.

2.3.2 Adsorption of H_2S

As mentioned earlier, H_2S is a toxic, corrosive gas and is one of the commonly seen contaminants present in several industrially essential feedstocks like coal gas, natural gas, liquefied petroleum gas, jet fuel and naphtha. H_2S is also a dominant source of acid rain, as the oxidation of H_2S causes the formation of sulfur oxide. Further, it can also poison several industrial catalysts like the supported nickel catalyst, which is employed in hydrocarbon steam reforming. Hence, the separation of H_2S from these liquid or gaseous streams is very essential. H_2S adsorption using different metal oxides or their mixtures has been explored in great details to overcome these challenges.

Metal oxides such as iron oxides are widely used for H_2S adsorption. These oxides separate H_2S by forming iron sulfides which are insoluble in nature.

The different chemical reactions occurring in this process are as described as follows:

$Fe_2O_3 + 3\ H_2S \rightarrow Fe_2S_3 + 3\ H_2O$
$Fe_2S_3 + 3/2\ O_2 \rightarrow Fe_2O_3 + 3\ S$

For the adsorption process, iron oxide is commonly employed in a form known as "iron sponge". The iron sponge consists of iron oxide (Fe_2O_3 and Fe_3O_4) impregnated wood chips, and can be used in batch as well as continuous systems. After the saturation, the sponge can be regenerated. However, after each regeneration cycle, the activity generally gets decreased by one-third [106]. In continuous system operation, the air is progressively added to the gaseous stream, and the regeneration of iron sponge occurs simultaneously. The H_2S removal rate is generally very high i.e., 2500 mg H_2S/g Fe_2O_3. However, the iron sponge has some disadvantages like high operating cost, chemically intensive process and production of continuous waste stream that might be either disposed of as dangerous waste or regenerated expensively. Some commercially generated iron oxide systems like Sulfatreat 410 HPR are available, which can produce non-hazardous waste. The adsorption capacity of Sulfatreat 410 HPR was reported to be 150 mg H_2S/g adsorbent [106]. Carnes *et al*. [107] reported that the metal oxide reactivities depend on intrinsic crystallite reactivity, crystallite size and the surface area. Further, it was also seen that when compared to the micro-crystalline structures, the nano-crystalline structures exhibited enhanced reactivity with H_2S. This is because of the higher surface area that promotes adsorption. Further, the presence of Fe_2O_3 enhanced the reaction due to the formation of iron sulfides which acted as the catalyst. Rodriguez and Maiti [108] reported that the H_2S adsorption ability of a metal oxide depended on the electronic band gap energy. More H_2S adsorption took place, when electronic band gap energy was less. This is due to the fact that the electronic bad gap is negatively related to oxide chemical reactivity. However, the reactivity depends on the mixing of oxide's bands with H_2S orbitals. In the case of better mixing, the oxides react well with sulfur containing molecules, thus forming metal sulfides. This causes the dissociation of H_2S molecules and sulfur immobilization in metal sulfides. In spite of this, the application of metal oxides for H_2S removal has some drawbacks like high cost, low selectivity, low separation effectiveness and lesser sorption/desorption rate.

At higher temperatures (200 °C - 400 °C), zinc oxide (ZnO) based materials are employed for removing H_2S traces. This is because, ZnO have better selec-

tivity for sulfides than the iron oxides [109]. Davidson *et al*. [109] conducted research on the H_2S removal capacity of ZnO, and it was observed that the ZnO surface reacted with H_2S to form a zinc sulfide insoluble layer, thus, separating the H_2S from the gas stream. Almost 40% of available H_2S was converted and the reaction depicted in the equation below led to the H_2S removal.

$ZnO + H_2S \rightarrow ZnS + H_2O$

Many commercial products have been developed employing ZnO, and the ultimate sulfur loading on these oxides materials has been observed in the range 300-400 mg S/g sorbent. Majority of research studies carried out till date for the advancement of solid H_2S adsorbents focused on the materials which are acceptable for higher temperatures (> 300 °C). Ca- and Fe-containing materials are among the most researched solid materials for H_2S removal from coal gas. This is because of their low cost and higher reactivity [110]. However, due to the presence of large amount of H_2 and large CO/CO_2 ratio in the coal gas, these materials have some disadvantages. For example, the Fe_3O_4 is reduced to FeO and Fe, however, the Fe_3C formed during the process decreases the sulfur uptake of the solid [111]. Lew *et al*. [112] also observed that ZnO was superior to iron oxide due to its agreeable sulfidation thermodynamics. However, the sulfidation kinetics of ZnO was slower than iron oxide. The major disadvantage of using ZnO based solid adsorbents for the application of hot gas cleaning is the damage which occurs because of the reduction of ZnO to elemental Zn which is volatile. Thus, a number of metal oxides have the potential for efficient use as gas adsorbents, however, many challenges are required to be resolved.

Several mixed metal oxides like Cu-Fe-O, Zn-Fe-V-O, Zn-V-O, Zn-Fe-Ti-O, Zn-Ti-O, Cu-Mo-O and Cu-Mn-O have been examined for the H_2S adsorption applications [113-116]. It was observed that the regeneration ability as well as reactivity got enhanced when these materials were deposited on an appropriate support. The mixed metal oxide $ZnFe_2O_4$ also exhibited good H_2S adsorption ability at higher temperature range of 500 °C – 700 °C [117]. For high temperature fuel gas desulfurization, Kobayshi *et al*. [118] examined the zinc ferrite silicon dioxide composites. Zinc ferrite was observed to undergo sulfidation in the reducing environment to form iron sulfides, zinc blende and wurtzite in the presence of 500 ppm of H_2S.

In another study, Huang *et al*. [119] studied the adsorption and reaction of H_2S on TiO_2 rutile (110) and anatase (101) surfaces using periodic density functional theory (DFT). The authors observed that H2S, HS, S, and H prefer-

entially adsorbed at the Ti_{5c}, O_{2c}, $(Ti_{5c})_2$, and O_{2c} sites, respectively, on the rutile surface, whereas these sites were Ti_{5c}, $(Ti_{5c})_2$, $(-O_{2c})(-Ti_{5c})$, and O_{2c}, respectively, on the anatase surface. Figure 2.10 also shows the adsorbed H_2S and the fragments HS, S and H on the TiO_2 rutile surface. Novochinskii *et al*. [120]

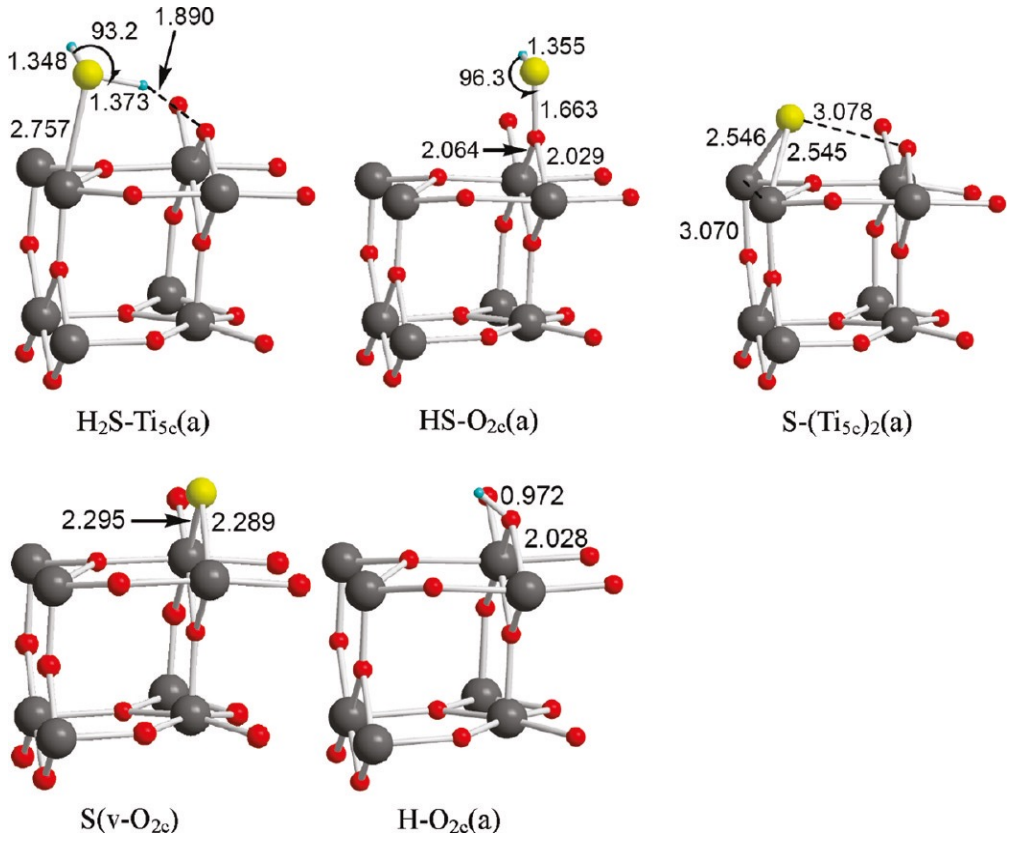

Figure 2.10 Geometries of adsorbed H_2S and its fragments, HS, S, and H, on the TiO_2 rutile (110) surface. Reproduced from Reference 119 with permission from American Chemical Society.

also reported a functional ZnO based adsorbent for low-temperature H_2S removal from steam-containing gas mixtures [120]. The authors observed very low H_2S outlet concentrations (20 parts per billion by volume) over the modified ZnO adsorbent. The authors observed the sulfur-trap capacity (which is the amount of H_2S trapped before breakthrough) to be dependent on factors such as space velocity, temperature, steam concentration, CO_2 concentration, and particle size. Figure 2.11 also demonstrates the performance of a ZnO-based trap at different concentrations of water vapor and H_2S. The authors observed higher trap capacity when the H_2S inlet concentration was higher. The trap capacity was also observed to decrease as a function of temperature. Presence of steam was noticed to inhibit the capture of H_2S by the adsorbent

due to the shifting of the equilibrium of the reaction. Furthermore, increasing the CO_2 concentration in the feed up to 12 vol % was also observed to decreases the capacity of ZnO for H_2S adsorption.

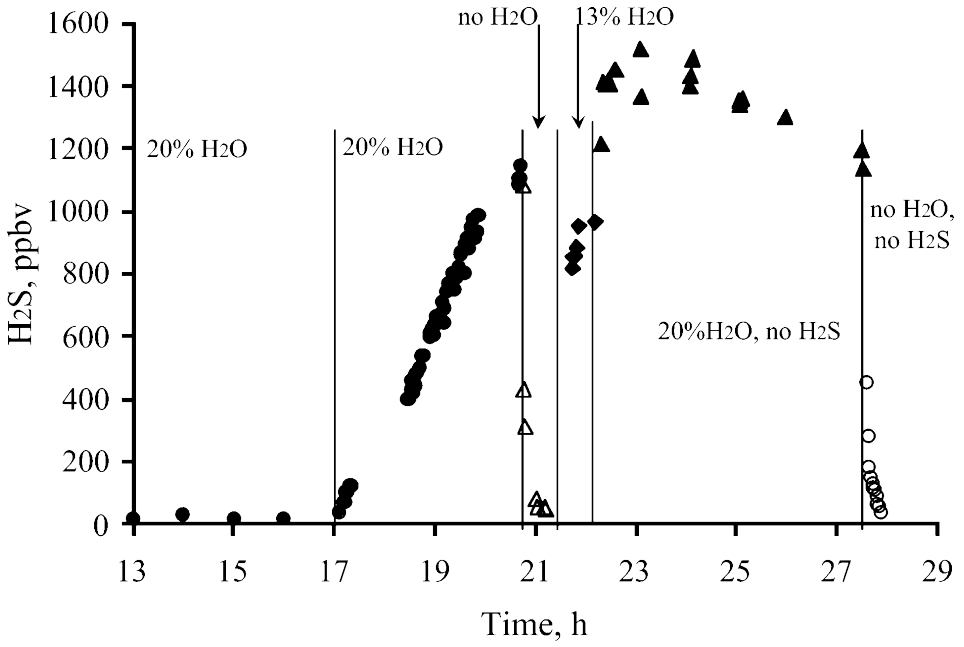

Figure 2.11 Performance of a ZnO-based trap at different concentrations of water vapor and H_2S. Reproduced from Reference 120 with permission from American Chemical Society.

For low temperature H_2S removal applications, several other studies have also been reported [107,109,121,122]. Carnes and Klabunde [107] examined the nano-crystalline metal oxides which were generated using sol gel technique. It was confirmed that at lesser temperature range (25 °C - 100 °C), the activity order was observed to be ZnO > CaO > Al2O3 >> MgO. Davidson *et al*. [109] examined the adsorption ability of H_2S using doped and high surface area ZnO at lower temperatures of 25 °C - 45 °C, and observed about 40% conversion of H_2S. Baird *et al*. [123] examined the ZnO doped with different oxides of Fe, Co and Cu, mixed Co–Zn oxides, Co-Zn-Al oxides, Co–Fe oxides to generate H_2S adsorbents at lower temperature. Out of the mixed metal oxides, Co-Zn oxide was reported to have the best H_2S adsorption ability at room temperature. Xue *et al*. [124] generated a series of pure metal oxides as well as mixed metal oxides from different hydrous oxides and hydroxy-carbonate precursors. It was observed that adsorbents like CuO, Zn/Co, Zn/Ti/Zr, Zn/Al and Zn/Mn mixed oxides exhibited good H_2S adsorption capacity at room temperature. The benefits of using hydroxycarbonate precursors included

good dispersion and a synergy of metal components which were expected to be continued in the mixed metal oxide succeeding calcination [125]. The high degree of dispersion of metal oxides is one of the most attractive feature of metal oxide based adsorbents for the low temperature performance. Some studies have also focused on the advancement of the mixed metal oxide adsorbents like Cu-Zn and Cu-Zn-Al for the H_2S adsorption at lower temperatures. These Cu based mixed metal oxides are considered to effective adsorbents for low temperature applications because of their low cost than the Zn–Co mixed metal-oxide adsorbents. However, the Cu based mixed oxides, which are generally reduced by hydrogen before being used as adsorbents, were also analyzed for the H_2S adsorption and some other organic sulfur compounds for middle or higher temperatures also [126,127]. Jiang *et al*. [128] generated a series of Cu-Zn hydroxy-carbonate precursors by co-precipitation method, with changing Cu/Zn molar ratios. In addition to this, two series of Cu-Zn-Al hydroxy-carbonate precursors were prepared with varying metal molar ratio, by co-precipitation as well as multi-precipitation methods. The high surface area Cu-Zn-Al metal oxides displayed remarkable sulfur removal capacities at the temperature range 25 °C - 100 °C. It was observed that for H_2S adsorption at low temperature, the Cu rich adsorbents were more suited than the Zn rich adsorbents. The probable reason for this behavior could be due to the fast sulfidation rate of CuO than ZnO because of the lesser rearrangement of anion lattice.

Polychronopoulou *et al*. [129] also studied the efficiency of mixed metal oxides Fe-Mn-Zn-Ti-O of differing composition, generated using sol gel technique, for the removal of H_2S from a gaseous mixture consisting of 7.5 vol % CO_2, 1-3 vol % H_2O, 25 vol % H_2 and 0.06 vol % H_2S, analyzed at temperature range 25 °C - 100 °C. The chemical interaction between the mixed metal oxide and H_2S was studied and it was observed that the molar ratio of Fe/Mn employed in the preparation of aforementioned metal oxides mostly determined the size and morphology of the generated solid particles. Comparison of the temperature effect on the H_2S adsorption for the sol gel generated 5Fe-15 Mn-40 Zn-40 Ti-O solid and the commercial nickel based solid was made in the presence of 1 vol % and 3 vol % H_2O in the feed stream. In the 1 vol % H_2O system, the commercial solid appeared to be better than the sol get generated mixed metal oxide at 25 °C - 100 °C temperature range. For the commercial solid, the H_2S adsorption enhanced by 141% by the increase in adsorption temperature from 25 °C - 100 °C. The presence of 1-3 vol % H_2O in the 7.5% CO_2/25% H_2/0.06% H_2S/He gas mixture remarkably increased the H_2S adsorption at 25 °C for 5 Fe-15 Mn-40 Zn-40 Ti-O solid.

In a recent study, in-situ formed graphene/ZnO nanostructured composites were employed for low temperature hydrogen sulfide removal from natural gas [130]. Nanostructured composites of graphene and highly dispersed sub-20 nm sized ZnO nanoparticles (TRGZ) were successfully prepared via by combining freeze-drying and thermal annealing processes. A series of compositions with different weight ratios of ZnO nanoparticles were prepared and used as a reactive sorbent in low temperature hydrogen sulfide (H_2S) removal from natural gas. The composite sorbent having a ZnO mass ratio of 45.1 wt% exhibited a significantly greater H_2S adsorption capacity (3.46 $mmol.g^{-1}$) than that of pure ZnO (1.06 $mmol.g^{-1}$), indicating that hybridization of ZnO with graphene significantly improved the H_2S removal ability. Figure 2.12 also shows the transmission elecrom micrographs (TEM) of (a) pristine ZnO nanoparticles, (b) TRGZ-1, (c) TRGZ-2, and (d) TRGZ-3 graphene/ZnO nanohybrids. The authors suggested that the possible mechanism involved initial physisorption of H_2S molecules with oxygenated functional groups of graphene which later can reach to the finely dispersed active ZnO nanoparticles and get chemisorbed through reactive adsorption. The EDX spectra of H_2S treated samples exhibited a strong peak for sulfur element indicating the reactive adsorption of H_2S on the sorbent.

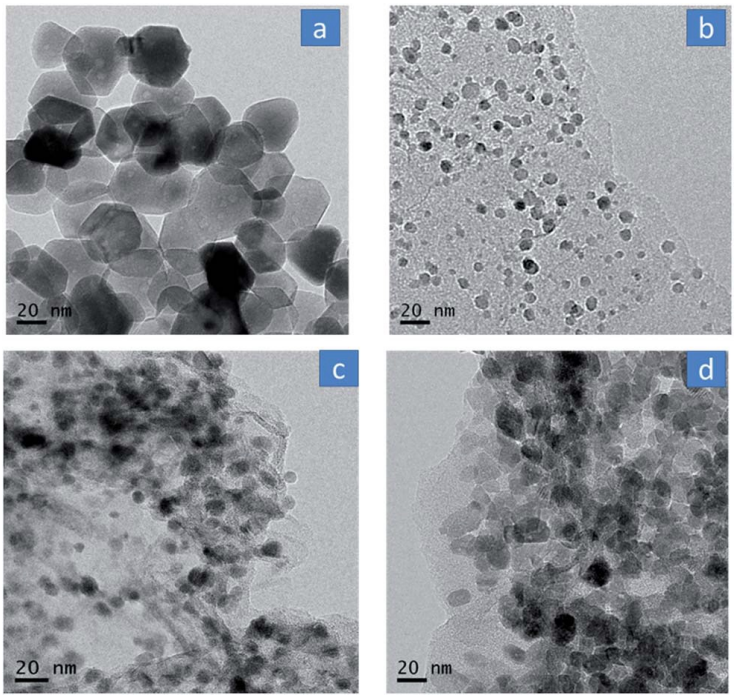

Figure 2.12 TEM images of (a) pristine ZnO nanoparticles, (b) TRGZ-1, (c) TRGZ-2, and (d) TRGZ-3 graphene/ZnO nanohybrids. Reproduced from Reference 130 with permission from Royal Society of Chemistry.

2.3.3 Adsorption of Organic Contaminants

Among the different physical methods employed for dye removal, adsorption is widely used method and considerable attention has been paid for the application of nano-sized adsorbent materials because of their higher surface area. In recent years, the utilization of magnetic particle technology for solving environmental issues has also gained attention. Different types of iron oxides have been studied for the dye adsorption, due to their reactive surface. These materials enable faster magnetic separation just after the adsorption. The magnetic particles can be employed for adsorbing the contaminants from gaseous or aqueous effluents and can subsequently be easily removed from the medium.

Luiz *et al*. [131] generated magnetic adsorbents by combining the magnetic properties of iron oxides and adsorption properties of the activated carbon. The iron oxide/activated carbon composites were used for the removal of volatile organic compounds like phenol, chloroform, drimaren red dye and chlorobenzene from the aqueous solution. It was noted that the existence of iron oxide did not influence the adsorption efficiency of activated carbon. In another study by Khosravi *et al*. [132], iron oxide nano-spheres were prepared using solvo-thermal method and were employed as an efficient adsorbent for anionic dye separation from the aqueous solution. Here, efficiency of iron oxide nano-spheres for the adsorption of anionic dyes namely reactive orange (RO) and reactive yellow (RY) was analyzed. The maximal adsorption capacity of RY and RO was observed to be 25.0 mg/g and 32.5 mg/g, respectively. The kinetic analysis confirmed rapid adsorption rate onto nano-spheres, which took place within 10 min. The adsorption process was exothermic and the optimum pH was about 4, i.e., acidic solution. At the final stage, due to the magnetic nature of the iron oxide nano-spheres, smooth separation from solution by a magnet could be achieved.

2.3.4 Heavy Metal Removal from Water/Wastewater

Heavy metal exposure, even at a very small level, is considered to be a danger for the living beings [133]. For the heavy metal separation from the water/wastewater, adsorption methods have become prominent techniques. Out of the various adsorbents available, nano-sized metal oxides (NMOs) are regarded as promising ones for the heavy metal removal from aqueous systems [134] .This is due to their greater surface areas as well as higher activities generated by the size quantization effect. The NMOs offer numerous ad-

vantages like preferable sorption, higher capacities and faster kinetics towards the heavy metals present in the water as well as wastewater. The examples for NMOs include nano-sized ferric oxides, aluminum oxides, magnesium oxides, manganese oxides, titanium oxides and cerium oxides. These materials exist in different forms such as tubes, particles, etc. On the other hand, when the metal oxide size decreases from the micrometer level to nanometer level, the enhancement in the surface energy causes poor stability. Hence, NMOs are prone to agglomeration because of the presence of van der Waals forces and other interactions, and thereby the high adsorption capacity as well as selectivity of NMOs can significantly reduce or even disappear [135]. Thus, the shape and size of these adsorbents are critical factors influencing their adsorption behavior.

The utilization of iron oxide based nano-materials is considered to be very effective for the separation of metal contaminants from water, due to their remarkable features such as small size, magnetic property, reusability and high surface area [136]. For instance, iron oxide nanomaterials exhibit excellent adsorption ability for the separation of arsenic from water. Feng *et al*. [137] generated super magnetic Fe_3O_4 coated with ascorbic acid, by hydrothermal process. The material had a surface area of 179 m^2/g and diameter < 10 nm. At room temperature, the material exhibited super paramagnetic behavior and the saturation magnetization attained 40 $emug^{-1}$, which indicated that these materials were suitable for use as an adsorbent for the separation of arsenic from waste water. The ultimate adsorption capacity of As(III) and As(V) was found to be 46.06 mg/g and 16.56 mg/g respectively.

The excessive application of copper in the industries leads to the accumulation in the environment, thereby polluting the water. Hao *et al*. [138] generated a magnetic nano-adsorbent (MNP-NH_2) by covalent binding of 1,6-hexadiamine on the Fe_3O_4 nanoparticles surface, and analyzed its adsorption capacity for the removal of copper ions from the aqueous solution. Different factors influencing the adsorption performance such as salinity, initial Cu^{2+} concentration, temperature, amount of MNP-NH_2, contact time and pH were examined. The magnetic nanoparticles were able to separate 98% of copper from tap water as well as the polluted water. It was noticed that the adsorption occurred faster and the equilibrium was attained within 5 min. The chemical sorption was noticed to be the rate limiting step of the sorption mechanism, and the ultimate adsorption ability was observed to be 25.77 $mg.g^{-1}$ at 298 K and pH value 6. The adsorbent MNP-NH_2 exhibited good resuability as well as higher stability under the experimental conditions. Complete desorption of the Cu^{2+} ions was achieved by using 0.1 $mol.L^{-1}$ HCl solution for < 1 min

and the regenerated MNP-NH_2 was able to retain the original metal discharge level. It was observed that the adsorption ability of the nano-adsorbent MNP-NH_2 remained constant, and no change in the desorption ability occurred during 15 adsorption - desorption cycles. In another study by Nashaat *et al*. [139], the adsorption mechanics, equilibria, thermodynamics and kinetics of Pb(II) ions onto Fe_3O_4 nano-adsorbents were analyzed. It was found that Fe_3O_4 nano-adsorbents had greater removal efficiency as Pb(II) was adsorbed from waste water in a very brief time and the equilibrium was accomplished within 30 min. Further, the adsorption was dependent on temperature, pH and the Pb(II) initial concentration. At pH value 5.5, the maximal removal of Pb(II) was obserevd. As the temperature and Pb(II) initial concentration was increased, the adsorption was also observed to enhance. The adsorption isotherms were determined using the Freundlich and Langmuir models. The thermodynamics of the adsorption of Pb(II) revealed the impulse nature, endothermic behavior and physisoprtion process. The regeneration as well as the desorption analysis confirmed the repeated use of nano-adsorbents without influencing the adsorption capacity. This confirmed the usefulness of Fe_3O_4 nano-adsorbents as inexpensive and effective adsorbents for the fast removal and recovery of the metal ions from wastewater.

The adsorptive behavior of nano-sized manganese oxides (NMnOs) are considered to be superior when compared to its bulk counterpart due to its greater surface area as well as polymorphic structures [140]. In the past several decades, NMnOs have been used for the sorption of anionic and cationic contaminants like arsenate, phosphate and heavy metal ions from natural water. Alumina (Al_2O_3) is also a conventional adsorbent for the removal of heavy metals and γ- $Al_2O_3$is regarded to be superior to α- Al_2O_3 in adsorption performance [141]. Nano-sized γ- Al_2O_3 adsorbents are generated using sol-gel method, and the materials have been used as solid phase extraction materials for the pre-concentration/separation of the trace metal ions. In the case of TiO_2, it was observed that the bulk and nano-TiO_2 differed in surface acidity, catalytic reactivity and chemical behavior, based on their various surface planes. From the BET analysis, it was seen that the nominal particle sizes were 8.3 and 329.8 nm, for nano-sized and bulk particles respectively [142]. The specific area of bulk particles was found to be 9.5 m^2/g, whereas the nanoparticles' specific area was 185.5 m^2/g. In a research study by Liang *et al*. [143], the nano-TiO_2 adsorbent, with BET surface area 208 m^2/g and diameter 10–50 nm exhibited adsorption capacity of Cd and Zn as 7.9 mg/g and 15.3 mg/g respectively at pH value 9. The effects of contact time, pH, interfering ions and elution solution on the adsorption performance of nano-TiO_2 for the

removal of Zn and Cd were examined. The presence of common anions and cations (in the concentration range of 100-5000 mg/L) was found to have no significant effect on the metal adsorption (Cd^{2+} ions and Zn^{2+} of 1.0 mg/mL) under the specified conditions. Many research studies have also confirmed the role of nano-structured ZnO to effectively remove the heavy metals from various media [144]. In a related study, Lee *et al*. [145] generated NZnOs powder using the solution combustion method. The authors observed that as compared with two TiO_2 powders, P25 and the other one generated by homogenous precipitation at lower temperature, the NZnO powder displayed greater Cu^{2+} adsorption from the solution.

Table 2.2 summarizes the heavy metals adsorption capacities of different metal oxides reviewed in this study.

Table 2.2 Heavy metal adsorption capacities of some of the metal oxide adsorbents

Sl. No.	Adsorbent	Temperature	pH value	Heavy metal	Adsorption capacity (mg/g)	Reference
1	Super-magnetic Fe_3O_4 coated with ascorbic acid	room temperature	-	As(III)	46.06 mg/g	115
2	Super-magnetic Fe_3O_4 coated with ascorbic acid	room temperature	-	As(V)	16.56 mg/g	115
3	Magnetic nano-adsorbent (MNP-NH_2)	298 K	6	Cu	25.77 mg/g	116
4	Nano-TiO_2 adsorbent		9	Cd	7.9 mg/g	103
5	Nano-TiO_2 adsorbent		9	Zn	15.3 mg/g	103

2.4 Summary and Outlook

Adsorption represents an immensely useful technology for the removal of harmful gases like H_2S, CO_2, SO_2, NH_3 present in the gas stocks and air as well as separation of organic contaminants and heavy metals from the wastewater. It has attracted remarkable consideration in both scientific exploration as well as commercial utilizations. Further, the development of state-of-the-art porous materials for the adsorption process is required to enhance the adsorption capacity or to overcome the existing disadvantages such as small pore volume or pore size of adsorbents. In this chapter, a comprehensive assessment on the use of MOFs and metal oxides for gas/vapor and liquid phase adsorptions has been presented. Further, focus has also been devoted to the

separation of a variety of contaminants like dyes and various heavy metals present in the water using the MOFs and metal oxides. As mentioned before, MOFs are promising adsorbents for the aforementioned applications due to their unique properties like higher surface area as well as tunable porosities. In addition to these properties, MOFs are able to consolidate functionalities by means of grafting or loading active or functional species and thereby increasing the adsorption capacity. Several modifications in MOFs, which were done in three aspects namely (1) metal ions, (2) organic liners and (3) novel consolidation of both, for enhancing the adsorption ability were also analyzed. The metal oxides exhibit enhanced selectivity because of the presence of chemical adsorption between the gas molecules and their surfaces. Both the surface area as well as pore size of the adsorbent greatly affects the gas diffusion in the adsorbent porous structure. Their reactivity depends on the crystallite size, intrinsic crystallite reactivity as well as the surface area. Nano sized metal oxides (NMOs) are considered to be an excellent adsorbent for the heavy metal removal from aqueous systems. In spite of the high adsorption capacity of the MOFs and metal oxides, there are several economical and technical barriers to promote the usage of these materials for gas adsorption and environmental applications. Most of these challenges are associated with material stability, remigration, high temperature performance, durability, loss of adsorption and selectivity, etc. However, with the employment of advanced nanotechnologies, it is envisaged that many of the currently existing limitations would be overcome in due course of time, which will pave the way for the large scale application of these MOFs and metal oxide materials for industrial and commercial applications.

References

1. Pawelec, B., Navarro, R. M., Campos-Martin, J. M., and Fierro, J. L. G. (2011) Towards near zero-sulfur liquid fuels: a perspective review. *Catalysis Science and Technology*, **1**, 23-42.
2. Vandenbroucke, A. M., Morent, R., Geyter, N. D., and Leys, C. (2011) Non-thermal plasmas for non-catalytic and catalytic VOC abatement. *Journal of Hazardous Materials*, **195**, 30-54.
3. Garces, H. F., Galindo, H. M., Garces, L. J., Hunt, J., Morey, A., and Suib, S. L. (2010) Low temperature H_2S dry-desulfurization with zinc oxide. *Microporous and Mesoporous Materials*, **127**, 190-197.
4. Petit, C., and Bandosz, T. J. (2010) Enhanced adsorption of ammonia on metal-organic framework/graphite oxide composites: analysis of surface interactions. *Advanced Functional Materials*, **20**, 111-118.

5. Colvile, R. N., Hutchinson, E. J., Mindell, J. S., and Warren, R. F. (2001) The transport sector as a source of air pollution. *Atmospheric Environment*, **30**, 1537-1565.
6. Bao, C., and Fang, C.-L. (2012) Water resources flows related to urbanization in china: challenges and perspectives for water management and urban development. *Water Resources Management*, **26**, 531-552.
7. Gupta, V. K., and Suhas (2009) Application of low-cost adsorbents for dye removal - a review. *Journal of Environmental Management*, **90**, 2313-2342.
8. Gong, Y., Zhao, X., Cai, Z., O'Reilly, S. E., Hao, X., and Zhao, D. (2014) A review of oil, dispersed oil and sediment interactions in the aquatic environment: influence on the fate, transport and remediation of oil spills. *Marine Pollution Bulletin*, **79**, 16-33.
9. Crini, G. (2006) Non-conventional low-cost adsorbents for dye removal: a review. *Bioresource Technology*, **97**, 1061-1085.
10. Chen, S., Zhang, J., Zhang, C., Yue, Q., Li, Y., and Li, C. (2010) Equilibrium and kinetic studies of methyl orange and methyl violet adsorption on activated carbon derived from phragmites australis. *Desalination*, **252**, 149-156.
11. Hasan, Z., Jeon, J., and Jhung, S. H. (2012) Adsorptive removal of naproxen and clofibric acid from water using metal-organic frameworks. *Journal of Hazardous Materials*, **209-210**, 151-157.
12. Ke, F., Qiu, L.-G., Yuan, Y.-P., Peng, F.-M., Jiang, X., Xie, A.-J., Shen, Y.-H., and Zhu, J.-F. (2011) Thiol-functionalization of metal-organic framework by a facile coordinationbased postsynthetic strategy and enhanced removal of Hg^{2+} from water. *Journal of Hazardous Materials*, **196**, 36-43.
13. Zhu, B.-J., Yu, X.-Y., Jia, Y., Peng, F.-M., Sun, B., Zhang, M.-Y., Luo, T., Liu, J.-H., and Huang, X.-J. (2012) Iron 1,3,5-benzenetricarboxylic metal-organic coordination polymers prepared by solvothermal method and their application in effcient As(V) removal from aqueous solutions. *Journal of Physical Chemistry C*, **116**, 8601–8607.
14. Li, J.-R., Sculley, J., and Zhou, H.-C. (2012) Metal- organic frame works for separations. *Chemical Reviews*, **112**, 869-932.
15. Babich, I. V., and Moulijn, J. A. (2003) Science and technology of novel processes for deep desulfurization of oil refinery streams: a review. *Fuel*, **82**, 607-631.
16. Velu, S., Ma, X., and Song, C. (2003) Selective adsorption for removing sulfur from jet fuel over zeolite-based adsorbents. *Industrial and Engineering Chemistry Research*, **42**, 5293-5304.
17. Choi, S., Drese, J.,H., and Jones, C. W. (2009) Adsorbent materials for carbon dioxide capture from large anthropogenic point sources. *ChemSusChem*, **2**, 796-854.
18. Zhou, A., Ma, X., and Song, C. S. (2006) Liquid-phase adsorption of multi-ring thiophenic sulfur compounds on carbon materials with different surface properties. *Journal of Physical Chemistry B*, **110**, 4699-4707.
19. Deliyanni, E., Seredych, M., and Bandosz, T. J. (2009) Interactions of 4,6-dimethyldibenzothiophene with the surface of activated carbons. *Langmuir*, **25**, 9302-9312.
20. Haque, E., Jun, J. W., Talapaneni, S. N., Vinu, A., and Jhung, S. H. (2010) Superior adsorption capacity of mesoporous carbon nitride with basic CN framework for phenol. *Journal of Materials Chemistry*, **20**, 10801-10803.

21. Wang, Y., Yang, R.,T., and Heinzel, J. M. (2008) Desulfurization of jet fuel by π-complexation adsorption with metal halides supported on MCM-41 and SBA-15 mesoporous materials. *Chemical Engineering Science*, **63**, 356-365.
22. Li, J.-R., Kuppler, R. J., and Zhou, H.-C. (2009) Selective gas adsorption and separation in metal-organic frameworks. *Chemical Society Reviews*, **38**, 1477-1504.
23. Jiang, H.-L., and Xu, Q. (2011) Porous metal-organic frameworks as platforms for functional applications. *Chemical Communications*, **47**, 3351-3370.
24. Seredych, M., and Bandosz, T .J. (2011) Removal of dibenzothiophenes from model diesel fuel on sulfur rich activated carbons. *Applied Catalysis, B: Environmental*, **106**, 133-141.
25. Ferey, G. (2008) Hybrid porous solids: past, present, future. *Chemical Society Reviews*, **37**, 191-214.
26. Sumida, K., Rogow, D. L., Mason, J. A., McDonald, T. M., Bloch, E. D., Herm, Z. R., Bae, T.-H., Long, J. R. (2012) Carbon dioxide capture in metal-organic frameworks. *Chemical Reviews*, **112**, 724-781.
27. Wu, H., Gong, Q., Olson, D. H., and Li, J. (2012) Commensurate adsorption of hydrocarbons and alcohols in microporous metal organic frameworks. *Chemical Reviews*, **112**, 836-868.
28. Suh, M. P., Park, H. J., Prasad, T. K., and Lim, D.-W. (2012) Hydrogen storage in metal-organic frameworks. *Chemical Reviews*, **112**, 782-835.
29. Li, J.-R., Sculley, J., and Zhou, H.-C. (2012) Metal-organic frameworks for separations. *Chemical Reviews*, **112**, 869-932.
30. Horcajada, P., Gref, R., Baati, T., Allan, P. K., Maurin, G., Couvreur, P., Ferey, G., Morris, R. E., and Serre, C. (2012) Metal-organic frameworks in biomedicine. *Chemical Reviews*, **112**, 1232-1268.
31. Furukawa, H., Ko, N., Go, Y. B., Aratani, N., Choi, S. B., Choi, E., Yazaydin, A. O., Snurr, R. Q., O'Keeffe, M., Kim, J., and Yaghi, O. M. (2010) Ultrahigh porosity in metal-organic frameworks. *Science*, **329**, 424-428.
32. Hamon, L., Serre, C., Devic, T., Loiseau, T., Millange, F., Ferey, G., and Weireld, G. D. (2009) Comparative study of hydrogen sulfide adsorption in the MIL-53(Al, Cr, Fe),MIL-47(V), MIL-100(Cr), and MIL-101(Cr) metal organic frameworks at room temperature, *Journal of American Chemical Society*, **131**, 8775-8777.
33. Hamon, L., Leclerc, H., Ghoufi, A., Oliviero, L., Travert, A., Lavalley, J.-C., Devic, T., Serre, C., Ferey, G., Weireld, G. D., Vimont, A., and Maurin, G. (2011) Molecular insight into the adsorption of H_2S in the flexible MIL-53(Cr) and rigid MIL-47(V) MOFs:infrared spectroscopy combined to molecular simulations. *Journal of Physical Chemistry C*, **115**, 2047-2056.
34. Liu, J., Thallapally, P. K., McGrail, B. P., and Brown, D. R. (2012) Progress in adsorption-based CO_2 capture by metal-organic frameworks. *Chemical Society Reviews*, **41**, 2308-2322.
35. Sumida, K., Rogow, D. L., Mason, J. A., McDonald, T. M., Bloch, E. D., Herm, Z. R., Bae, T.-H., and Long, J. R. (2012) Carbon dioxide capture in metal-organic frameworks. *Chemical Reviews*, **112**, 724-781.
36. Dathe, H., Peringer, E., Roberts, V., Jentys, A., and Lercher, J. A. (2005) Metal organic frameworks based on Cu^{2+} and benzene-1,3,5-tricarboxylate as host for SO_2 trapping agents. *C. R. Chimie*, **8**, 753-763.

37. Planchais, A., Devautour-Vinot, S., Giret, S., Salles, F., Trens, P., Fateeva, A., Devic, T., Yot, P., Serre, C., Ramsahye, N,m and Maurin, G. (2013) Adsorption of benzene in the cation-containing MOFs MIL-141. *Journal of Physical Chemistry C*, **117**(38), 19393-19401.
38. Huxford, R. C., Rocca, J. D., and Lin W. (2010) Metal-organic frameworks as potential drug carriers. *Current Opinion in Chemical Biology*, **14(2)**, 262-268.
39. Kitagawa, S., Kitaura, R., and Noro, S.-I. (2004) Functional porous coordination polymers. *Angewandte Chemie International Edition*, **43**, 2334-2375.
40. Cavka, J. H., Jakobsen, S., Olsbye, U., Guillou, N., Lamberti, C., Bordiga, S., and Lillerud, K. P. (2008) A new zirconium inorganic building brick forming metal organic frameworks with exceptional stability. *Journal of American Chemical Society*, **130**, 13850-13851.
41. Walton, K. S., Millward, A. R., Dubbeldam, D., Frost, H., Low, J. J., Yaghi, O. M., and Snurr, R. Q. (2008) Understanding inflections and steps in carbon dioxide adsorption isotherms in metal-organic frameworks. *Journal of American Chemical Society*, **130**, 406-407.
42. Demessence, A., D'Alessandro, D. M., Foo, M. L., and Long, J. R. (2009) Strong CO_2 binding in a water-stable, triazolate-bridged metal-organic framework functionalized with ethylenediamine. *Journal of American Chemical Society*, **131**, 8784-8786.
43. Britt, D., Furukawa, H., Wang, B., Glover, T. G., and Yaghi, O. M. (2009) Highly efficient separation of carbon dioxide by a metal-organic framework replete with open metal sites. *Proceedings of the National Academy of Sciences of the USA*, **106**, 20637-20640.
44. Dietzel, P. D. C., Besikiotis, V., and Blom, R. (2009) Application of metal-organic frameworks with coordinatively unsaturated metal sites in storage and separation of methane and carbon dioxide. *Journal of Materials Chemistry*, **19**, 7362-7370.
45. Caskey, S. R., Wong-Foy, A. G., and Matzger, A. J. (2008) Dramatic tuning of carbon dioxide uptake via metal substitution in a coordination polymer with cylindrical pores. *Journal of American Chemical Society*, **130**, 10870-10871.
46. Couck, S., Denayer, J. F. M., Baron, G. V., Remy, T., Gascon, J., and Kapteijn, F. (2009) An amine-functionalized MIL-53 metal-organic framework with large separation power for CO_2 and CH_4. *Journal of American Chemical Society*, **131**, 6326-6327.
47. Bae, Y. S., Farha, O. K., Spokoyny, A. M., Mirkin, C. A., Hupp, J. T., and Snurr, R. Q. (2008) Carborane-based metal-organic frameworks as highly selective sorbents for CO_2 over methane. *Chemical Communications*, **37**, 4135-4137.
48. Hayashi, H., Cote, A. P., Furukawa, H., O'Keeffe, M., and Yaghi, O. M. (2007) Zeolite A imidazolate frameworks. *Nature Materials*, **6**, 501-506.
49. Phan, A., Doonan, C. J., Uribe-romo, F. J., Knobler, C. B., O'Keeffe, M., and Yaghi, O. M. (2010) Synthesis, structure, and carbon dioxide capture properties of zeolitic imidazolate frameworks. *Accounts of Chemical Research*, **43**, 58-67.
50. Hu, Z., Khurana, M., Seah, Y. H., Zhang, M., Guo, Z., and Zhao, D. (2015) Ionized Zr-MOFs for highly efficient post-combustion CO_2 capture, *Chemical Engineering Science*, **124**, 61-69.
51. Hu, Z. G., Zhang, K., Zhang, M., Guo, Z. G., Jiang, J. W., and Zhao, D. (2014) A

combinatorial approach towards water stable metal-organic frameworks forhighl efficient carbon dioxide separation. *ChemSusChem*, **7**, 2791-2795.
52. Yang, D.-A., Cho, H.-Y., Kim, J., Yang, S.-T., and Ahn, W.-S. (2012) CO_2 capture and conversion using Mg-MOF-74 prepared by a sonochemical method. *Energy & Environmental Science*, **5**, 6465-6473.
53. Achmann, S., Hagen, G., Hammerle, M., Malkowsky, I. M., Kiener, C., and Moos, R. (2010) Sulfur removal from low-sulfur gasoline and diesel fuel by metal-organic frameworks. *Chemical Engineering & Technology*, **33**, 275-280.
54. Chavan, S., Bonino, F., Valenzano, L., Civalleri, B., Lamberti, C., Acerbi, N., Cavka, J. H., Leistner, M., and Bordiga, S. (2013) Fundamental aspects of H_2S adsorption on CPO-27-Ni. *Journal of Physical Chemistry C*, **117**, 15615-15622.
55. van de Voorde, B., Hezinova, M., Lannoeye, J., Vandekerkhove, A., Marszalek, B., Gil, B., Beurroies, I., Nachtigall, P., and De Vos, D. (2015) Adsorptive desulfurization with CPO-27/MOF-74: an experimental and computational investigation. *Physical Chemistry and Chemical Physics*, **17**, 10759-10766.
56. Hamon, L., Serre, C., Devic, T., Loiseau, T., Millange, F., Frrey, G., and De Weireld, G. (2009) Comparative study of hydrogen sulfide adsorption in the MIL-53 (Al, Cr Fe), MIL-47 (V), MIL-100 (Cr), and MIL-101 (Cr) metal-organic frameworks at room temperature. *Journal of American Chemical Society*, **131**, 8775-8777.
57. Hamon, L., Leclerc, H., Ghoufi, A., Oliviero, L., Travert, A., Lavalley, J. C., Devic, T., Serre, C., Ferey, G., De Weireld, G., Vimont, A., and Maurin, G. (2011) Molecular in-sight into the adsorption of H_2S in the flexible MIL-53 (Cr) and rigid MIL-47 (V) MOFs: infrared spectroscopy combined to molecular simulations. *Journal of Physical Chemistry C*, **115**, 2047-2056.
58. Chen, Z., Ling, L., Wang, B., Fan, H., Shangguan, J., and Mi, J. (2016) Adsorptive desulfurization with metal-organic frameworks: A density functional theory investigation. *Applied Surface Science*, **387**, 483-490.
59. Fernandez, C. A., Thallapally, P. K., Motkuri, R.,K., Nune, S. K., Sumrak, J. C., Tian, J., and Liu, J. (2010) Gas-induced expansion and contraction of a fluorinated metal-organic framework. *Crystal Growth & Design*, **10**, 1037-1039.
60. Ahmed, I., and Jhung, S. H. (2014) Composites of metal-organic frameworks: preparation and application in adsorption. *Materials Today*, **17**, 136-146.
61. Glover, T. G., Peterson, G. W., Schindler, B. J., Britt, D., and Yaghi, O. M. (2011) MOF-74 building unit has a direct impact on toxic gas adsorption. *Chemical Engineering Science*, **66**, 163-170.
62. Petit, C., and Bandosz, T. J. (2012) Exploring the coordination chemistry of MOF-graphite oxide composites and their applications as adsorbents. *Dalton Transactions*, **41**, 4027-4035.
63. Britt, D., Tranchemontagne, D., and Yaghi, O. M. (2008) Metal-organic frameworks with high capacity and selectivity for harmful gases. *Proceedings of the National Academy of Sciences of the USA*, **105**, 11623–11627.
64. Karra, J. R., and Walton, K. S. (2008) Effect of open metal sites on adsorption of polar and nonpolar molecules in metal organic framework Cu-BTC. *Langmuir*, **24**, 8620-8626.
65. Xiao, B., Wheatley, P. S., Zhao, X., Fletcher, A. J., Fox, S., Rossi, A. G., Megson, I. L.,

Bordiga, S., Regli, L., Thomas, K. M., and Morris, R. E. (2007) High-capacity hydrogen and nitric oxide adsorption and storage in a metal organic framework. *Journal of American Chemical Society*, **129**, 1203-1209.

66. Jhung, S. H., Lee, J.-H., Yoon, J. W., Serre, C., Ferey, G., Chang, J.-S. (2007) Microwave synthesis of chromium terephthalate MIL-101 and its benzene sorption ability. *Advanced Materials*, **19**, 121-124.
67. Shi, J., Zhao, Z., Xia, Q., Li, Y., Li, Z. (2011) Adsorption and diffusion of ethyl acetate on the chromium-based metal-organic framework MIL-101. *Journal of Chemical Engineering Data*, **56**, 3419-3425.
68. Taylor, J. M., Vaidhyanathan, R., Iremonger, S. S., and Shimizu, G. K. H. (2012) Enhancing water stability of metal- organic frameworks via phosphonatemonoester linkers. *Journal of American Chemical Society*, **134**, 14338–14340.
69. Greathouse, J. A., and Allendorf, M. D. (2006) The interaction of water with MOF-5 simulated by molecular dynamics. *Journal of American Chemical Society*, **128**, 10678-10679.
70. Der Voort, P. V., Leus, K., Liu, Y.-Y., Vandichel, M., Speybroeck, V. V., Waroquier, M., and Biswas, S. (2014) Vanadium metal-organic frameworks: structures and applications. *New Journal of Chemistry*, **34**, 1853-1867.
71. Valenzano, L., Civalleri, B., Chavan, S., Bordiga, S., Nilsen, M. H., Jakobsen, S., Lillerud, K. P., and Lamberti, C. (2011) Disclosing the complex structure of UiO-66 metal organic framework: A synergic combination of experiment and theory. *Chemistry of Materials*, **23**(7), 1700-1718.
72. Park, K. S., Ni, Z., Cote, A. P., Choi, J. Y., Huang, R., Uribe-Romo, F. J., Chae, H. K., O'Keeffe, M., and Yaghi, O. M. (2006) Exceptional chemical and thermal stability of zeolitic imidazolate frameworks. *Proceedings of the National Academy of Sciences of the USA*, **103**, 10186-10191.
73. Ehrenmann, J., Henninger, S.,K., and Janiak, C. (2011) Water adsorption characteristics of mil-101 for heat-transformation applications of MOFs. European Journal of Inorganic Chemistry, 2011(4), DOI: doi:10.1002/ejic.201190006.
74. Jeremias, F., Khutia, A., Henninger, S. K., and Janiak, C. (2012) MIL-100(Al, Fe) as water adsorbents for heat transformation purposes - a promising application. *Journal of Materials Chemistry*, **22**, 10148-10151.
75. Cychosz, K. A., and Matzger, A. J. (2010) Water stability of microporous coordination polymers and the adsorption of pharmaceuticals from water. *Langmuir*, **26**, 17198-17202.
76. Wu, T., Shen, L., Luebbers, M., Hu, C., Chen, Q., Ni, Z., and Masel, R. I. (2010) Enhancing the stability of metal-organic frameworks in humid air by incorporating water repellent functional groups. *Chemical Communications*, **46**, 6120-6122.
77. Zu, D.-D., Lu, L., Liu, X.-Q., Zhang, D.-Y., and Sun, L.-B. (2014) Improving hydrothermal stability and catalytic activity of metal-organic frameworks by graphite oxide incorporation. *The Journal of Physical Chemistry C*, **118**, 19910-19917.
78. Yang, C., Kaipa, U., Mather, Q. Z., Wang, X., Nesterov, V., Venero, A. F., and Omary, M. A. (2011) Fluorous metalorganic frameworks with superior adsorption and hydrophobic properties toward oil spill cleanup and hydrocarbon storage. *Journal of the American Chemical Society*, **133**, 18094-18097.

79. Hasan, Z., and Jhung, S. H. (2015) Removal of hazardous organics from water using metal-organic frameworks (MOFs): Plausible mechanisms for selective adsorptions. *Journal of Hazardous Materials*, **283**, 329-339.
80. Haque, E., Lee, J. E., Jang, I. T., Hwang, Y. K., Chang, J.-S., Jegal, J., and Jhung, S. H. (2010) Adsorptive removal of methyl orange from aqueous solution with metal-organic frameworks, porous chromium-benzenedicarboxylates. *Journal of Hazardous Materials*, **181**, 535-542.
81. Haque, E., Lo, V., Minett, A. I., Harris, A. T., and Church, T. L. (2014) Dichotomous adsorption behaviour of dyes on an amino-functionalised metal-organic framework, amino-MIL-101(Al). *Journal of Materials Chemistry A*, **2**, 193-203.
82. Haque, E., Jun, J. W., and Jhung, S. H. (2011) Adsorptive removal of methyl orange and methylene blue from aqueous solution with a metal-organic frame- work material, iron terephthalate (MOF-235). *Journal of Hazardous Materials*, **185**, 507-511.
83. Leng, F., Wang, W., Zhao, X. J., Hu, X. L., and Li, Y. F. (2014) Adsorption interaction between a metal-organic framework of chromium–benzenedicarboxylates and uranine in aqueous solution. *Colloids & Surfaces A*, **441**, 164-169.
84. Chen, C., Zhang, M., Guan, Q., and Li, W. (2012) Kinetic and thermodynamic studies on the adsorption of xylenol orange onto, MIL-101(Cr). *Chemical Engineering Journal*, **183**, 60-67.
85. Liu, B., Yang, F., Zou, Y., and Peng, Y. (2014) Adsorption of phenol and p-nitrophenol from aqueous solutions on, metal-organic frameworks: effect of hydrogen bonding. *Journal of Chemical Engineering Data*, **59**, 1476-1482.
86. Xie, L., Liu, D., Huang, H., Yang, Q., and Zhong, C. (2014) Efficient capture of nitrobenzene from waste water using metal-organic frameworks. *Chemical Engineering Journal*, **246**, 142-149.
87. Khan, N. A., Jung, B. K., Hasan, Z., and Jhung, S. H. (2015) Adsorption and removal of phthalic acid and diethylphthalate from water with zeolitic imidazolate and metal-organic frameworks. *Journal of Hazardous Materials*, **282**, 194-200.
88. Tong, M., Liu, D., Yang, Q., Devautour-Vinot, S., Maurin, G., and Zhong, C. (2013) Influence of framework metal ions on the dye capture behavior of MIL-100 (Fe, Cr) MOF type solids. *Journal of Materials Chemistry A*, **1**, 8534-8537.
89. Wang, H.-N., Liu, F.-H., Wang, X.-L., Shao, K.-Z., and Su, Z.-M. (2013) Three neutral metal-organic frameworks with micro and meso-pores for adsorption and separation of dyes. *Journal of Materials Chemistry A*, **1**, 13060-13063
90. Han, R., Zou, W., Wang, Y., and Zhu, L. (2007) Removal of uranium (VI) from aqueous solutions by manganese oxide coated zeolite: discussion of adsorption isotherms and pH effect. *Journal of Environmental Radioactivity*, **93**, 127-143.
91. Feng, Y., Jiang, H., Li, S., Wang, J., Jing, X., Wang, Y., and Chen, M. (2013) Metal–organic frameworks HKUST-1 for liquid-phase adsorption of Uranium. *Colloids and Surfaces A*, **431**, 87-92.
92. Batzill, M. (2012) The surface science of graphene: Metal interfaces, CVD synthesis, nanoribbons, chemical modifications, and defects. *Surface Science Reports*, **67**, 83-115.
93. Furukawa, H., Cordova, K. E., O'Keeffe, M., and Yaghi, O. M. (2013) The chemistry and applications of metal-organic frameworks. *Science*, **341**, 1230444-1230456.

94. Tao, X., Ma, W., Li, J., Huang, Y., Zhao, J., and Yu, J. C. (2003) Efficient degradation of organic pollutants mediated by immobilized iron tetrasulfophthalocyanine under visible light irradiation. *Chemical Communications*, 80-81.
95. Kyzas, G. Z., and Matis, K. A. (2015) Nanoadsorbents for pollutants removal: a review. *Journal of Molecular Liquids*, **203**, 159-168.
96. House, K. Z., Harvey, C. F., Aziz, M. J., and Schrag, D. P. (2009) The energy penalty of post-combustion CO_2 capture & storage and its implications for retrofitting the U.S. installed base. *Energy & Environmental Science*, **2**, 193-205.
97. Cai, W., Yu, J., Anand, C., Vinu, A., and Jaroniec, M. (2011) Facile synthesis of ordered mesoporous alumina and alumina-supported metal oxides with tailored adsorption and framework properties. *Chemistry of Materials*, **23**, 1147-1157.
98. Leon, M., Diaz, E., Bennici, S., Vega, A., Ordonez, S., and Auroux, A. (2010) Adsorption of CO_2 on hydrotalcite-derived mixed oxides: Sorption mechanisms and consequences for adsorption irreversibility. *Industrial and Engineering Chemistry Research*, **49**, 3663-3671.
99. Yoshikawa, K., Sato, H., Kaneeda, M., and Kondo, J. N. (2014) Synthesis and analysis of CO_2 adsorbents based on cerium oxide. *Journal of CO_2 Utilization*, **8**, 34-38.
100. Wang, X. P., Yu, J. J., Cheng, J., Hao, Z. P. and Xu, Z. P. (2008) High-temperature adsorption of carbon dioxide on mixed oxides derived from hydrotalcite-like compounds. *Environmental Science and Technology*, **42**, 614-618.
101. Zhao, Z., Dai, H., Du, Y., Deng, J., Zhang, L., and Shi, F. (2011) Solvo- or hydrothermal fabrication and excellent carbon dioxide adsorption behaviors of magnesium oxides with multiple morphologies and porous structures. *Materials Chemistry and Physics*, **128**, 348-356.
102. Song, G., Zhu, X., Chen, R., Liao, Q., Ding, Y.-D., and Chen, L. (2016) An investigation of CO_2 adsorption kinetics on porous magnesium oxide. *Chemical Engineering Journal*, **283**, 175-183.
103. Kumar, S., Saxena, S. K., Drozd, V., and Durygin, A. (2015) An experimental investigation of mesoporous MgO as a potential pre-combustion CO_2 sorbent. *Materials for Renewable and Sustainable Energy*, **4**:8, DOI: 10.1007/s40243-015-0050-0.
104. Vu, A. T., Park, Y., Jeon, P. R., and Lee, C. H. (2014) Mesoporous MgO sorbent promoted with KNO_3 for CO_2 capture at intermediate temperatures. *Chemical Engineering Journal*, **258**, 254-264.
105. Ding, Y.-D., Song, G., Liao, Q., Zhu, X., and Chen, R. (2016) Bench scale study of CO_2 adsorption performance of MgO in the presence of water vapor. *Energy*, **112**, 101-110.
106. Abatzoglou, N., and Boivin, S. (2009) A review of biogas purification processes. *Biofuels, Bioproducts and Biorefining*, **3**, 42-71.
107. Carnes, C. L., Klabunde, K. J. (2002) Unique chemical reactivities of nanocrystalline metal oxides toward hydrogen sulfide. *Chemistry of Materials*, **14**, 1806-1811.
108. Rodriguez, J. A., and Maiti, A. (2000) Adsorption and decomposition of H_2S on MgO(100), NiMgO(100), and ZnO(0001) surfaces: A first-principles density functional study. *The Journal of Physical Chemistry B*, **104**, 3630-3638.
109. Davidson, J. M., Lawrie, C. H., and Sohail, K. (1995) Kinetics of the absorption of

hydrogen sulfide by high purity and doped surface area zinc oxide. *Industrial and Engineering Chemistry Research*, **34**, 2981-2989.
110. Ozdemir, S., and Bardakci, T. (1999) Hydrogen sulfide removal from coal gas by zinc titanate sorbent. *Separation and Purification Technology*, **16**, 225-234.
111. Ayala, R. E., and Marsh, D. W. (1991) Characterization and long-range reactivity of zinc ferrite in high-temperature desulfurization processes. *Industrial and Engineering Chemistry Research*, **30**, 55-60.
112. Lew, S., Jothimurugesan, K., and Stephanopoulos, M. F. (1992) The reaction of zinc titanate and zinc oxides solids. *Chemical Engineering Science*, **47**, 1421-1431.
113. Woods, M. C., Gangwal, S. K., Harrison, D. P., and Jothimurugesan, K. (1991) Kinetic of the reactions of a zinc ferrite sorbent in high-temperature coal gas desulfurization. *Industrial and Engineering Chemistry Research*, **30**, 100-107.
114. Akyurtlu, J. F., and Akyurtlu, A. (1995) Hot gas desulfurization with vanadium-promoted zinc ferrite sorbents. *Gas Separation and Purification*, **9**, 17-25.
115. Tamhankar, S. S., Bagajewicz, M., Gavalas, G. R., Sharma, P. K., and Flytzani-Stephanopoulos, M. (1986) Mixed-oxide sorbents for high- temperature removal of hydrogen sulfide. *Industrial and Engineering Chemistry Process Design and Development*, **25**, 429-437.
116. Flytzani-Stephanopoulos, M., Gavalas, G. R., and Tamhankar, S. S. (1998) High Temperature Regenerative H_2S Sorbents, US Patent 4729889.
117. Focht, G. D., Ranade, P. V., and Harrison, D. P. (1988) High-temperature desulfurization using zinc ferrite: Reduction and sulfidation kinetics. *Chemical Engineering Science*, **48**(11), 3005-3013.
118. Kobayashi, H., Shirai, M., and Nunokawa, M. (2002) High-temperature sulfidation behavior of reduced zinc ferrite in simulated coal gas revealed by in situ X-ray diffraction analysis and Mossbauer spectroscopy. *Energy & Fuels*, **16**, 601-607.
119. Huang, W.-F., Chen, H.-T., and Lin, M. C. (2009) Density functional theory study of the adsorption and reaction of H_2S on TiO_2 Rutile (110) and anatase (101) surfaces. *The Journal of Physical Chemistry C*, **113**, 20411-20420.
120. Novochinskii, I. I., Song, C., Ma, X., Liu, X., Shore, L., Lampert, J., and Farruato, R. J. (2004) Low-temperature H_2S removal from steam-containing gas mixtures with ZnO for fuel cell application. 1. ZnO particles and extrudates. *Energy & Fuels*, **18**, 576-583.
121. Bagreev, A., Rahman, H., and Bandosz, T. J. (2001) Thermal regeneration of activated carbon previously used as hydrogen sulfide adsorbent. *Carbon*, **39**, 1319-1326.
122. Polychronopoulou, K., Fierro, J. L. G., and Efstathiou, A. M. (2004) Novel Zn-Ti-based mixed metal oxides for low-temperature adsorption of H_2S from industrial gas streams. Applied Catalysis B: Environmental, 57, 125-137.
123. Baird, T., Campbell, K. C., Holliman, P. J., Hoyle, R., Noble, G., Stirling, D., and Williams, B. P. (2003) Mixed cobalt–iron oxide absorbents for low-temperature gas desulfurization. *Journal of Materials Chemistry*, **13**, 2341-2347.
124. Xue, M., Chitrakar, R., Sakane, K., and Ooi, K. (2003) Screening of adsorbents for removal of H_2S at room temperature. *Green Chemistry*, **5**, 529-534.
125. Bems, B., Schur, M., Dassenoy, A., Junkes, H., Herein, D., and Schlogl, R. (2003) Relations between synthesis and microstructural properties of copper/zinc hydroxycarbonates. *Chemistry - A European Journal*, **9**, 2039-2052.

126. Karvan, O., Sirkecioglu, A., and Atakul, H. (2009) Investigation of nano-CuO/mesoporous SiO2 materials as hot gas desulphurization sorbents. *Fuel Processing Technology*, **90**, 1452-1458.
127. Bae, J. W., Kang, S. H., Dhar, G. M., and Jun, K. W. (2009) Effect of Al_2O_3 content on the adsorptive properties of $Cu/ZnO/Al_2O_3$ for removal of odorant sulfur compounds. *International Journal of Hydrogen Energy*, **34**, 8733-8740.
128. Jiang, D., Su, L., Ma, L., Yao, N., Xu, X., Tang, H., and Li, X. (2010) Cu–Zn–Al mixed metal oxides derived from hydroxycarbonate precursors for H_2S removal at low temperature. *Applied Surface Science*, **256**, 3216-3223.
129. Polychronopoulou, K., Galisteo, F. C., Granados, M. L., Fierro, J. L. G., Bakas, T., and Efstathiou, A. M. (2005) Novel Fe–Mn–Zn–Ti–O mixed-metal oxides for the low-temperature removal of H2S from gas streams in the presence of H_2, CO_2, and H_2O. *Journal of Catalysis*, **236**, 205-220.
130. Lonkar, S. P., Pillai, V., Abdala, A., and Mittal, V. (2016) In situ formed graphene/ZnO nanostructured composites for low temperature hydrogen sulfide removal from natural gas. *RSC Advances*, **6**, 81142-81150.
131. Oliveira, L. C. A., Rios, R. V. R. A., Fabris, J. D., Garg, V., Sapag, K., and Lago, R. M. (2002) Activated carbon/ iron oxide magnetic composites for the adsorption of contaminants in water. *Carbon*, **40**, 2177-2183.
132. Khosravi, M., and Azizian, S. (2014) Adsorption of anionic dyes from aqueous solution by iron oxide nanospheres. *Journal of Industrial and Engineering Chemistry*, **20**, 2561-2567.
133. Tchounwou, P. B., Yedjou, C. G., Patlolla, A. K., and Sutton, D. J. (2012) Heavy metals toxicity and the environment. *EXS*, **101**, 133-164.
134. Agrawal, A., and Sahu, K. K. (2006) Kinetic and isotherm studies of cadmium adsorption on manganese nodule residue. *Journal of Hazardous Materials*, **137**, 915-924.
135. Pradeep, T., and Anshup (2009) Noble metal nanoparticles for water purification: A critical review. *Thin Solid Films*, **517**, 6441-6478.
136. Warner, C. L., Chouyyok, W., Mackie, K. E., Neiner, D., Saraf, L. V., Droubay, T. C., Warner, M. G., and Addleman, R. S. (2012) Manganese doping of magnetic iron oxide nanoparticles: tailoring surface reactivity for a regenerable heavy metal sorbent. *Langmuir*, **28**(8), 3931-3937.
137. Feng, L., Cao, M., Ma, X., Zhu, Y., and Hu, C. (2012) Superparamagnetic high-surface-area Fe_3O_4 nanoparticles as adsorbents for arsenic removal. *Journal of Hazardous Materials*, **217-218**, 439-446.
138. Hao, Y.-M., Man, C., and Hu, Z.-B. (2010) Effective removal of Cu (II) ions from aqueous solution by amino-functionalized magnetic nanoparticles. *Journal of Hazardous Materials*, **184**(1-3), 392-399.
139. Nassar, N. N. (2010) Rapid removal and recovery of Pb(II) from wastewater by magnetic nanoadsorbents. *Journal of Hazardous Materials*, **184**(1-3), 538-546.
140. Wang, H. Q., Yang, G. F., Li, Q. Y., Zhong, X. X., Wang, F. P., Li, Z. S., and Li, Y. H. (2011) Porous nano- MnO_2: large scale synthesis via a facile quick-redox procedure and application in a supercapacitor. *New Journal of Chemistry*, **35**, 469-475.

141. Li, J. D., Shi, Y. L., Cai, Y. Q., Mou, S. F., and Jiang, G. B. (2008) Adsorption of di-ethyl-phthalate from aqueous solutions with surfactant-coated nano/microsized alumina. *Chemical Engineering Journal*, **140**, 214-220.
142. Engates, K. E., and Shipley, H. J. (2011) Adsorption of Pb, Cd, Cu, Zn, and Ni to titanium diox-ide nanoparticles: effect of particle size, solid concentration, and exhaustion. *Environmental Science and Pollution Research*, **18**, 386-395.
143. Liang, P., Shi, T. Q., and Li, J. (2004) Nanometer-size titanium dioxide separation/preconcentration and FAAS determination of trace Zn and Cd in water sample. *International Journal of Environmental Analytical Chemistry*, **84**, 315-321.
144. Wang, X. B., Cai, W. P., Lin, Y. X., Wang, G. Z., and Liang, C. H. (2010) Mass production of micro/nanostructured porous ZnO plates and their strong structurally enhanced and selective adsorption performance for environmental remediation. *Journal of Materials Chemistry*, **20**, 8582-8590.
145. Lee, J. H., Kim, B. S., Lee, J. C., and Park, S. (2005) Removal of Cu++ ions from aqueous Cu-EDTA solution using ZnO nanopowder. In: *Eco-Materials Processing & Design VI*, Kim, H. S., Park, S.-Y., Hur, B. Y., and Lee, S. W. (eds.), Trans Tech Publications, Korea, pp. 510-513.